Biochemical Pharmacology, Vol. 40, No. 1, pp. 97–113, 1990.
Printed in Great Britain.

0006-2952/90 \$3.00 + 0.00

NMR STUDIES OF AN OLIGONUCLEOTIDE WITH AN UNUSUAL STRUCTURE INDUCED BY PLATINUM ANTI-CANCER DRUGS

TAMMY PAGE KLINE,[*] LUIGI G. MARZILLI,[*†‡] DAVID LIVE[*†] and GERALD ZON[§]
[*]Department of Chemistry, Emory University, Atlanta, GA 30322; and [§]Applied Biosystems, Foster City, CA 94404, U.S.A.

Abstract—The ^{31}P NMR spectra of $Pt(en)\{d(T_1A_2T_3G_4G_5G_6T_7A_8C_9C_{10}C_{11}A_{12}T_{13}A_{14})\}$ (14-mer) and $Pt(en)\{d(A_2T_3G_4G_5G_6T_7A_8C_9C_{10}C_{11}A_{12}T_{13})\}$ (12-mer) (en = ethylenediamine) each contain two signals far downfield (*ca.* −2.9 and −2.6 ppm from trimethylphosphate standard), two signals slightly downfield, and at least one signal slightly upfield of the normal range (*ca.* −4.0 to −4.4 ppm). This pattern suggested a distorted structure. The unusual ^{31}P signals of the 12-mer were assigned by analogy to signals of the 14-mer previously assigned by ^{17}O-labeling methods. A combination of heteronuclear multiple-quantum coherence, one-dimensional and two-dimensional nuclear Overhauser effect (1D- and 2D-NOE) and homonuclear shift correlation spectroscopy (COSY) experiments assigned all aromatic ^1H signals of the 12-mer except H8 of G_5 or G_6. One of these H8 signals is missing from the spectrum and the nucleotide is labeled G_m. The other H8 is the most downfield signal and has a strong NOE to its H1′. Since this strong NOE indicates that this nucleoside exists in a *syn* conformation, it is labeled G_s. A strong NOE was observed between the G_s and A_8 H8 signals. Several lines of evidence suggested a hairpin-like structure with a loop region ($G_6T_7A_8C_9$) and a stem region involving $A_2T_3G_4G_5$ and $C_{10}C_{11}A_{12}T_{13}$. The ^{31}P signals for the stem region are within or slightly outside the normal range. $^3J_{H3'\text{-}P}$ values (3–6 Hz), measured by a 2D-*J* experiment, of stem nucleotides were characteristic for a DNA duplex. Imino signals for base pairs A_2T_{13}, T_3A_{12}, G_4C_{11}, and probably G_5C_{10}, and the observation of internucleotide NOE connectivities for these nucleotides (e.g. between an H8 signal and the H1′ signal of the 5′ nucleotide) suggested a right-handed helical structure. For the loop region, a distorted sugar-phosphate backbone is indicated by far downfield positions of the G_5pG_6 and A_8pC_9 ^{31}P signals, the $^3J_{H3'\text{-}P}$ values for C_9p (8.0 Hz) and A_8p (6.8 Hz), and the absence of H3′-P coupling for G_5p. In the loop region, no imino signals or internucleotide NOEs characteristic of a right-handed duplex were observed. However, A_8H8, C_9H6, and C_{10}H6 each exhibited unusual internucleotide NOEs to the H4′ signal of the 5′ residue. NOE crosspeaks between T_7 ^1H signals and signals attributed to sugars of the G_s and G_m suggested that the T_7 moiety is located within the space encircled by the loop. The few NOE crosspeaks, pH dependence, and Cu^{2+} broadening of C_9 ^1H signals indicate an isolated location accessible to solvent. Selective reverse chemical shift correlation, 1D- and 2D-NOE, and COSY experiments for the 14-mer produced results very similar to those described above for the 12-mer. We evaluated the following four models for the structure of the loop region of the 12-mer and the 14-mer: (1) Model I, in which Pt is bound to G_5G_6; (2) Model II, in which Pt is bound to three bases, G_5, G_6, and A_8; (3) a variation of Model II (Model IIC), in which one of the G bases forms a Pt—C8 bond; and (4) Model III, in which Pt is bound to A_8 and either G_5 or G_6. Model I does not explain the NOE between the A_8 and G_s H8 signals nor the missing H8 signal. Two sets of results provide evidence against Model II and Model IIC. First, the ^{195}Pt NMR spectra of the 12-mer and 14-mer have signals (−2645 and −2640 ppm respectively) similar to the reported shift for $(Pt(en)(Guo)_2\text{-}N7,N7)^{2+}$. Second, the presence of all fifteen signals in the 9–7 ppm region for 12-mer after Pt removal by KCN in D_2O suggested that Pt does not bind at C8. Model III provides the best explanation for our results. A pH dependence study of the 12-mer tentatively assigned G_s as G_5. In summary, we believe that Model III, in which Pt binds G_5, is most reasonable and that a bend may occur at the intersection of the loop and stem regions.

The primary molecular target of *cis*$Pt(NH_3)_2Cl_2$, a widely used anti-cancer drug, is believed to be DNA [1–3]. The binding preference of *cis*$Pt(NH_3)_2Cl_2$ for mixtures of nucleotide monophosphates, under physiological conditions, is G N7 > A N7 ⩾ A N1 ≥ C N3 [1]. Evidence indicates that an intrastrand GpG crosslink is the predominant adduct formed by this drug and the analogous species, $Pt(en\|)Cl_2$ [1]. ^{31}P and ^1H NMR spectral studies of polynucleotides, oligodeoxyribonucleotides (oligomers), and mononucleotides treated with anti-tumor active Pt drugs (*cis*PtA_2Cl_2) have been employed to examine the structural consequences on the phosphate-ribose backbone and base conformation after Pt binding [1–17].

^{31}P NMR spectroscopy has demonstrated that active (e.g. *cis*$Pt(NH_3)_2Cl_2$), but not inactive (e.g. *trans*$Pt(NH_3)_2Cl_2$), compounds induce an unusual downfield ^{31}P NMR signal in DNA [6, 7], nucleosomes [6], polynucleotides [6, 8], and oligonucleo-

---

[†] L. G. M. and D. L. are also members of the Winship Cancer Center.

[‡] Corresponding author.

[||] Abbreviations: en, ethylenediamine; TEA A, triethylammonium acetate buffer; PIPES, 1,4-piperazinebis-(ethanesulfonic acid); TRIS, tris(hydroxymethyl)aminomethane; NOE, nuclear Overhauser effect; COSY, homonuclear shift correlation spectroscopy; 2D NMR, two-dimensional nuclear magnetic resonance; HMQC, heteronuclear multiple-quantum coherence; HMBC, heteronuclear multiple-bond coherence; SRCSC, selective reverse chemical shift correlation; and CD, circular dichroism.

tides [4, 7, 9–11, 13, 14] containing adjacent 6-oxopurine bases. For a series of self-complementary oligomers treated with *cis*PtA_2Cl_2 drugs, downfield signals were observed only when GpG was present in the sequence [9]. ^{31}P–^1H Decoupling or ^{17}O-labeling experiments with *cis*PtA_2\{d(TCTCGGTCTC)-N7(5),N7(6)\} [2, 3, 7] and HMQC and ^{17}O-labeling studies with *cis*PtA_2\{d(TGGT)-N7(2),N7(3)\} [4, 13] established that the ^{31}P signal of the Pt intrastrand GpG crosslink is shifted downfield to *ca.* −3 ppm. For both oligomers, the shift of this downfield signal correlated with the potential hydrogen bonding ability of the *cis*PtA_2 moiety [2, 3, 13]. X-Ray structures of *cis*$Pt(NH_3)_2$ adducts of di- and trinucleotides, and molecular mechanics calculations of *cis*$Pt(NH_3)_2$ adducts of oligonucleotides indicate that hydrogen bonding between an amine ligand on Pt and the phosphate 5′ to the GpG binding site is an important feature of Pt binding [1–3].

^1H NMR spectroscopy has provided considerable insight into ribose and base conformations of *cis*PtA_2Cl_2-treated oligomers and polynucleotides [1]. Certain structural characteristics have been found for Pt crosslinked GpG residues. Specifically, it has been determined that the adjacent bases are linked via N7, and NOE experiments with *cis*PtA_2 adducts of poly(I)-poly(C) [8], d(TCTCGGTCTC) [16], and d(TGGT) [4, 13] revealed that the adjacent purines are in a head-to-head configuration and that the adjacent G residues are in an *anti* conformation.

In recent studies, several techniques, particularly 1D ^1H and ^{31}P NMR spectroscopy, were used to investigate the reaction of the self-complementary tetradecadeoxyribonucleotide (14-mer) $d(TATGGGTACCCATA)_2$ with $Pt(en)Cl_2$ [15, 17]. The ^{31}P NMR spectrum of Pt(en)\{d(TATGGGTACCCATA)\} revealed two signals far downfield, two signals slightly downfield, and two signals slightly upfield of the normal range for DNA ^{31}P signals. All ^{31}P NMR signals for this platinated oligomer were assigned by ^{17}O-labeling methods [15, 17]. The far downfield signals at *ca.* −2.6 and −2.9 ppm were assigned as A_8pC_9 and G_5pG_6, respectively, suggesting an unusual conformation for the ribose-phosphate backbone. The ^{31}P NMR spectrum of a shorter 10-mer analogue, Pt(en)\{d(TGGGTACCCA)\}, has the same unusual ^{31}P spectral features as that of the platinated 14-mer [15, 17]. ^{17}O-Labeling assignments of the far downfield signals for this 10-mer were consistent with those of the longer analogue [15]. Further evidence for an unusual structure for these platinated oligomers is the absence of one H8 signal. Additional studies, including ^1H NMR spectroscopy, UV absorbance, electrophoresis, and CD spectroscopy suggested a hairpin-like structure in which the 5′ region TATG hydrogen bonds with the 3′ end CATA and the loop containing the sequence GGTAC is stabilized by hydrogen bonds between the amine groups on the Pt and the oligonucleotide [15, 17]. The similarity of the ^{31}P NMR spectrum of the 10-mer to that of the 14-mer indicated that a long stem region is not a necessary component of the structure. An initial model (Model I) was proposed in which the Pt is bound at the G_5pG_6 site. The missing signal was unexplained [15, 17].

The unprecedented nature of these results was intriguing. Furthermore, the remarkable high yield formation of one product is surprising, given the alternative binding sites (two GpG, one GpNpG, one ApNpG, one GpNpA, one ApNpA, and one GpNpNpA), and we have continued to investigate this system. A more detailed understanding of the structure of Pt(en)\{d(TATGGGTACCCATA)\} could conceivably reveal yet unrecognized aspects of Pt–DNA interactions. Additionally, the elucidation of this structure represented a significant challenge to modern NMR methods. The current study suggests that the binding site is actually GpNpNpA and that the bound G residue exists in a *syn* conformation, both unprecedented results.

EXPERIMENTAL

Materials

Oligodeoxyribonucleotides (oligomers) were prepared by the phosphoramidite method and purified as described previously [2, 3]. Solution concentrations were determined spectrophotometrically at 260 nm using a molar extinction coefficient of $\varepsilon = 6300\ M^{-1}\ cm^{-1}$.

Pt *reactions*

Solutions of the Pt complexes (synthesized as described previously [2, 3]) were prepared by adding 4 mg of the Pt compound to H_2O (1 mL) or PIPES 10 buffer (0.010 M PIPES, 0.100 M $NaNO_3$, 0.001 M EDTA, pH 7.0) (1 mL) and heating the mixture at 60° until dissolution. Appropriate volumes of the Pt solutions were added to samples of $d(TATGGGTACCCATA)_2$ or $d(ATGGGTACCCAT)_2$ (0.020 M bases, H_2O or PIPES 10 buffer, 10^{-4} M EDTA, pH 7). Samples were maintained at 12° for approximately 1 week. Reactions were checked for completeness by ^1H NMR.

After platination, 2D NMR samples were purified by HPLC on a Hamilton PRP-1 (0.7 × 30.5 cm) column. Eluent A was 0.1 M TEA A and eluent B was HPLC-UV grade CH_3CN. The gradient employed was 9–12% in 14 min and 12–15% in 3 min. The major product (≥90% total area) eluted at 12 min and was collected, lyophilized, and dissolved in H_2O. Minor products eluted later. To remove TEA A, the solution of the major product was passed through a 2 × 20 cm Sephadex G-10 column once or twice and, if necessary, passed over Dowex (Na^+ form). To prepare a D_2O sample for 2D NMR, the purified sample was dissolved in D_2O, lyophilized, and redissolved in D_2O. The pH was then adjusted to 7.0. The lyophilization–D_2O dissolution cycle was repeated two to three times. The sample was kept *in vacuum* until exposed to nitrogen in a glove bag, where it was dissolved in 99.996% D_2O (0.5 mL) and transferred to an NMR tube.

KCN addition

An aliquot of a 0.30 M KCN solution was added to solutions of Pt(en)\{d(ATGGGTACCCAT)\} in H_2O and D_2O to a final ratio of CN^-/Pt of 30. The reaction was monitored by electrophoresis and ^1H NMR spectroscopy. The same experiment was conducted on a solution of Pt(en){d(TATGGGTACCCATA)} in D_2O. The final product of this reaction was purified by HPLC and analyzed by an enzyme digest method described previously [18].

Instrumental methods

One-dimensional NMR spectroscopy. (a) *^1H NMR.* Spectra were obtained at 361 MHz with a Nicolet 360-NB spectrometer or at 500 MHz with a GN-500 spectrometer each equipped with a variable temperature unit. Typical conditions for recording spectra of D_2O solutions include: 5000 Hz sweep-width, 30° pulse width, 64 scans, 0.3 Hz line broadening, and 16K data points. For H_2O/D_2O samples, a version of the 1331 pulse sequence [2, 3] was employed with typical conditions: 15,000 Hz sweep-width, 32 scans, 1.0 Hz line broadening, and 16K data points. Sample conditions were typically 0.03 M, pH 6.8, 0.5 mL volume, 99.9% D_2O or 90% H_2O:10% H_2O in 5-mm NMR tubes. D_2O was purchased from Aldrich. TSP [$(CH_3)_3SiCD_2CD_2COONa$ from Aldrich] was used as an internal reference.

(b) *1D NOE.* A 1331 solvent suppression pulse sequence with presaturation was used. The presaturation time was 300 msec. One hundred scans were accumulated in an interleaving mode of 5 cycles, irradiating on and off the resonance of interest, resulting in a total of 500 total scans for each.

(c) *^{31}P NMR.* Spectra were obtained at 81 MHz with an IBM WP-200SY spectrometer or at 202 MHz with a GN-500 spectrometer each equipped with a variable temperature unit. Typical conditions for recording spectra with the IBM WP-200SY include 1300 Hz sweep width, 45° pulse width, 10,000 scans. 1.0 Hz line broadening, and 4K data points. GN-500 conditions include 1000 Hz sweep width, 45° pulse width, 200 scans, 1.0 Hz line broadening, and 4K data points. ^1H NMR samples, contained in 5-mm NMR tubes, were concentrically placed in 10-mm NMR tubes with the identical solvent surrounding the insert. A small amount of TMP [$(CH_3O)_3PO$ from Aldrich] was added to the 10-mm tube as a reference.

(d) *^{195}Pt NMR.* Spectra were obtained at 107 MHz on a GN-500 spectrometer equipped with a 10-mm broad band probe and a 12-bit ADC. Typical conditions for recording spectra include 142,857 Hz sweep width, 45° pulse width, 50 Hz line broadening, 1024 data points, and 3.58 msec acquisition time. Eight separate acquisitions of 1,048,565 scans each in double precision mode were obtained and then block averaged. Sample conditions were 0.030 M (0.003 M Pt), pH 7.0, 0.5 mL, 99.9% D_2O in a 5-mm NMR tube. A 0.1 M solution of Na_2PtCl_6 was used as the reference.

Two-dimensional NMR spectroscopy. The following experiments were performed with the GE GN-500 spectrometer equipped for reverse detection experiments.

(a) *^1H–^{31}P HMQC.* The pulse sequence used was $90(^1H)$-$1/2J_{HP}$-$90(^{31}P)$-$t_1/2$-$180(^1H)$-$t_1/2$-$90(^{31}P)$-acquire(^1H) [4, 19]. The $1/2J$ delay was set at 50 msec. The ^1H sweep width was 3012 Hz in 512 points for an acquisition time of 0.26 sec. A repetition delay of 1.3 sec was used. One hundred twenty-eight blocks of 128 scans were collected. The sweep width in the ^{31}P dimension as 1706 Hz with an effective acquisition time of 42.6 msec. The ^{31}P dimension was zero-filled once before processing. Data are displayed in absolute value mode.

(b) *Selective reverse chemical shift correlation (SRCSC).* The pulse sequence for this experiment was: saturation(^1H)-$90(^{31}P)$-$t_1/2$-$180_{sel}(^1H)$-$180(^1H)$-$t_1/2$-$90(^{31}P)$-$90(^1H)$-aquire(^1H) [20] (t_1 is the evolution time in the ^{31}P dimension). The sweep width in the ^1H dimension was 1300 Hz in 1024 points for an acquisition time of 787 msec. One hundred twenty-eight blocks of 64 scans each were collected. The power of the selective pulse was 125 Hz (in units of $\gamma H/2\pi$) with the transmitter set at 4.8 ppm. Alternate scans were stored in separate areas of memory and processed to yield a phased 2D spectrum [20, 21]. The sweep width in the ^{31}P dimension was 300 Hz with an effective acquisition time in that dimension of 426 msec. The ^{31}P dimension was zero-filled twice before processing, and the resulting phased 2D spectrum, including both positive and negative contours, is shown. This experiment selects for H3′-P correlations, and the splitting of the signal in the ^{31}P dimension is the result of vicinal coupling between these nuclei. Spectral range in the ^{31}P dimension was reduced to increase digital resolution resulting in the folding over of peaks downfield of −3 ppm.

(c) *2D-J.* Experimental conditions were $90(^1H)$-$t_1/2$-$90_{sel}(^1H)$-$180(^{31}P)$-$90_{sel}(^1H)$-$t_1/2$-acquire(^1H)-decouple(^{31}P) [20]. The ^1H sweep width was 1300 Hz with a size of 1024 points for an acquisition time of 787 msec. Sixty-four blocks of 64 scans each were collected. The magnitude of the selective pulse was 119 Hz centered at 4.75 ppm. The spectral width in the f_1 dimension was 50 Hz with an effective acquisition time of 1.28 sec. The f_1 dimension was zero-filled twice before processing. Data are presented in phased mode.

(d) *NOESY.* The pulse sequence used was 90°-t_1-90°-τ_m-90°-acquire [22, 23]. A mixing time of 700 msec and a sweepwidth of 5000 Hz in both dimensions were used. Five hundred twelve blocks of 32 scans and 1024 data points each were collected at 12° and 22°.

(e) *COSY.* The pulse sequence used was 90°-t_1-90°-acquire. A sweep width of 5000 Hz in both dimensions was used. Five hundred twelve blocks of 16 scans and 1024 data points were collected at 12° and 22°.

HPLC. HPLC purifications and analyses were performed as described previously [2, 3] on Rainin Rabbit Gradient HPLC systems with either a Hitachi 100-30 spectrophotometer set at 260 nm or an LDC/Milton Roy "uvMonitor" spectrophometer equipped with a 254 nm photo-cell cartridge.

UV Spectroscopy. Melting experiments were performed with a Perkin–Elmer Lambda 3B spectrophotometer equipped with an electronically heated 5-cell holder, temperature controller, and temperature programmer. A solution containing 0.1 mM Pt(en){d(ATGGGTACCCAT)} in PIPES 10 buffer was placed in a sealed cuvette with a 1-cm path length. A second cuvette contained the reference buffer. The thermistor was placed in this cuvette to record sample temperature. The temperature was increased at a rate of 0.5°/min. The temperature (5 to 95°) and absorbance values (260 nm) were recorded every 2 min.

Electrophoresis. Polyacrylamide gel electrophoresis was performed as described previously [2, 3].

RESULTS

The simplicity of the 1D ^{1}H and ^{31}P NMR spectra as well as UV and electrophoretic analysis indicate the formation of only one major product for the 14-mer and the 12-mer [15, 17] when treated with $Pt(en)Cl_2$. The 14-mer is numbered in the following manner:

Pt(en){d(T A T G G G T A C C C A T A)}
1 2 3 4 5 6 7 8 9 10 11 12 13 14

To remain consistent with the numbering scheme of the Pt(en){d(TATGGGTACCCATA)}, we number its twelve-base analogue (12-mer) as follows:

Pt(en){d(A T G G G T A C C C A T)}
2 3 4 5 6 7 8 9 10 11 12 13

The combination of only one reaction product and more than one downfield ^{31}P NMR signal is indicative of some type of unusual structure formed by platination that produces remote effects on phosphate groups other than the binding site. Other analytical methods were employed in order to gain a better understanding of the nature of the structure of Pt(en){d(TATGGGTACCCATA)} [15, 17]. Several lines of evidence, among them CD spectroscopy, UV melting profiles, electrophoretic mobility, and ^{1}H NMR spectroscopy in H_2O, indicate that the 14-mer is not a duplex. Although the system has many properties similar to those of a hairpin, there are enough differences that the term "hairpin-like" would be more appropriate here.

In the following, assignments of the ^{1}H NMR signals of Pt(en){d(TATGGGTACCCATA)} and Pt(en){d(ATGGGTACCCAT)} are made. The aromatic signals of all bases are identified except for G_5 and G_6. One of these two nucleosides is in a *syn* conformation and has a broad downfield H8 signal. The H8 signal of the other base is missing from the aromatic region. In making assignments for the sugar, amino, and imino protons of these two nucleotides, the designations G_5 and G_6 are used when evidence suggests the specific identity (i.e. H3′, amino, and imino signals). The terms G_s and G_m are used if it is only known whether the proton is on the nucleotide of the *syn* G or the G with the missing H8 signal respectively (i.e. H1′, H2′/H2″, and H4′). As mentioned above, previous studies had suggested a hairpin-like structure for the 14-mer and 10-mer [17]. For the 1D NOE studies in H_2O, it was thus assumed that a stem region exists in which T_1 base pairs with A_{14} to form T_1A_{14}, A_2 base pairs with T_{13} to form A_2T_{13}, and so on.

Most of the ^{1}H NMR assignments by 2D methods were made on the 12-mer. ^{31}P NMR spectroscopy and ^{31}P–^{1}H heteronuclear methods were important in the assignments. Results on the 12-mer are presented first. Subsequently, some additional assignments were made with the 14-mer, and these results are presented second.

Pt(en){d(ATGGGTACCCAT)} (12-mer) Results

^{31}P NMR Spectroscopy. The ^{31}P NMR spectrum (25°, PIPES 10) of the 12-mer exhibits the same pattern as that of 14-mer [15, 17] (see ^{31}P spectra in Figs. 1 and 2 and Table 1). By analogy with the ^{17}O labeling assignments made for the 14-mer, signal assignments are as follows: A_8pC_9 (−2.45 ppm); G_5pG_6 (−2.83 ppm); G_6pT_7 (−3.55 ppm); T_3pG_4 (−3.67 ppm); and T_7pA_8 (−4.65 ppm). Only one slightly upfield signal was observed for the 12-mer, whereas two were observed for the 14-mer (T_7pA_8 and A_2pT_3). Since T_1 and A_{14} are absent, A_2pT_3 is now at the 5′ end, and it is assumed that its signal occurs in the main signal cluster for the 12-mer. This assumption is supported by 2D NMR studies (see below). The ^{31}P NMR spectrum of a solution of Pt(en){d(ATGGGTACCCAT)} containing no salt was similar except for the shifting of the G_6pT_7 and T_3pG_4 signals to −3.67 ppm, where they overlap.

^{1}H NMR Spectroscopy. 9 to 7 ppm Region. The aromatic region of Pt(en){d(ATGGGTACCCAT)} exhibits characteristics previously observed for the 14-mer [15, 17]. (Fig. 3). First, two broad signals are shifted downfield. This type of signal is typical of the H8 of platinated guanine bases in single-stranded oligonucleotides. Second, fifteen signals should be present in this region, but only fourteen are observed. Thus, one signal is missing in this region.

15 to 10 ppm Region. This region of the ^{1}H NMR spectrum of Pt(en){d(ATGGGTACCCAT)} (10% D_2O, pH 7.0, 0.030 M, 5°) has sharp signals at 13.67, 13.08, and 12.67 ppm. Two moderately broad resonances are evident at 13.00 and 11.97 ppm and one very broad resonance at ~11 ppm. Decreasing the pH to 6.1 caused the signal at 11.97 ppm to sharpen. The broad signal at ~11 ppm also sharpened slightly. No change was observed for the other signals. The spectrum of this region at pH 6.1, shown in Fig. 4, was recorded at 10°, a temperature at which the A_2T_3 signal occurs at a more isolated position.

Assignments. (a) H3′, T H6, A H8, G H8. 2D NOE and COSY experiments were conducted on a solution of Pt(en){d(ATGGGTACCCAT)} (pH 7.0, 0.030 M, 12°). Many connectivities typical of duplexed DNA molecules were missing. However, by a combination of NOESY and COSY, nonspecific assignments of aromatic signals were made. For this system, a mixing time of 700 msec gave the best results. Experiments using shorter mixing times of 250 and 500 msec produced only crosspeaks also observed in the τ_m = 700 msec experiment, only fewer. NOESY and COSY connectivities are seen between the T methyl groups and the three most upfield singlets in the aromatic region, thus assigning these signals at T H6s. T H6 signals are typically the furthest upfield in the aromatic region. The three C H6 doublets are easily identified. The three singlets between 7.8 and 8.1 ppm have no clear NOE crosspeaks to other signals and are especially sharp, both characteristics of A H2 signals. The remaining five signals are assigned as H8s. Since there should be

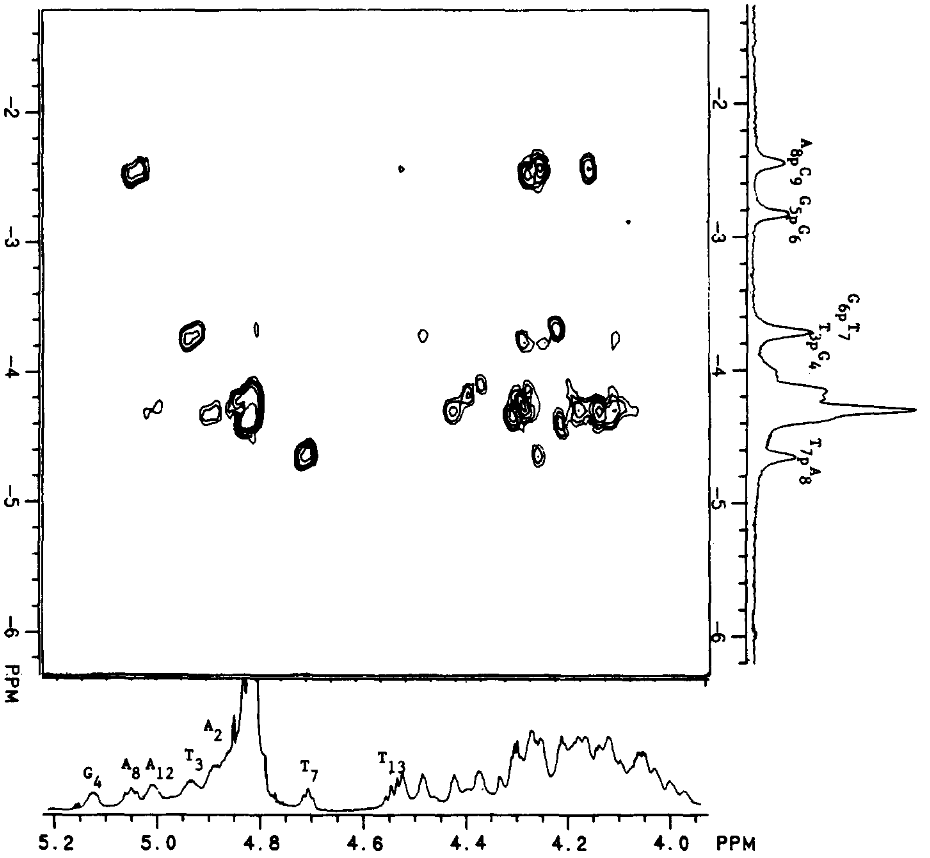

Fig. 1. A section of the contour plot of a ^1H–^{31}P HMQC experiment on the platinated oligonucleotide Pt(en){d($A_2T_3G_4G_6T_7A_8C_9C_{10}C_{11}A_{12}T_{13}$)} (0.002 M, 99.9% D_2O, 10^{-4} M EDTA, pH 7, 21°).

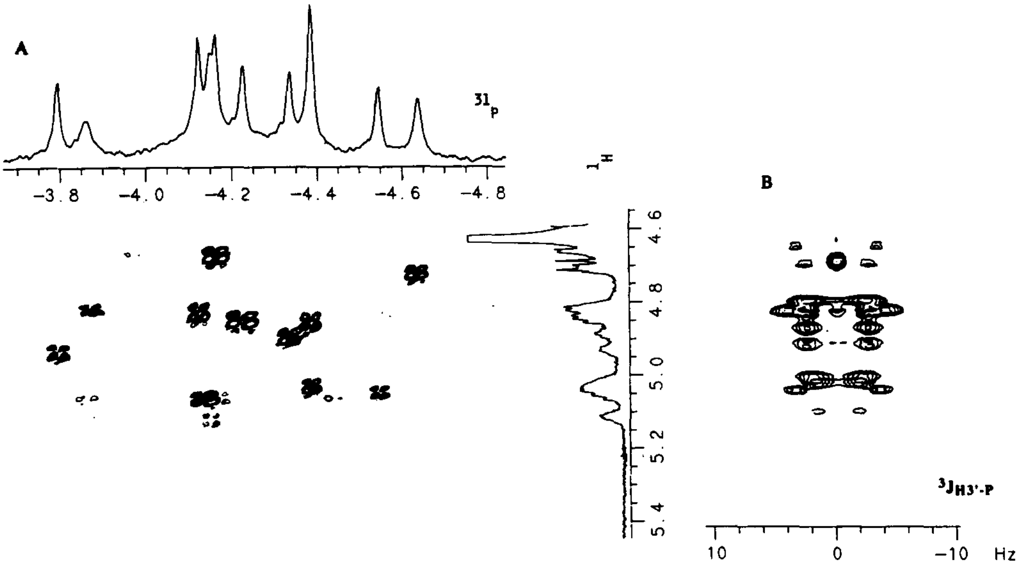

Fig. 2. Sections of the contour plots of (A) ^1H detected ^1H–^{31}P selective reverse chemical shift correlation experiment and (B) ^1H detected ^1H–^{31}P heteronuclear 2D *J* correlation map of Pt(en){d($T_1A_2T_3G_4G_5G_6T_7A_8C_9C_{10}C_{11}A_{12}T_{13}A_{14}$)} (0.003 M, 99.9% D_2O, 10^{-4} M EDTA, pH 7, 40°). Normal 1D ^1H and ^{31}P spectra are shown along respective axes (in units of ppm) for reference. In order to increase digital resolution in the ^{31}P dimension, the sweep width in this dimension was reduced, causing the lowest field ^{31}P resonance at −2.65 ppm to appear at *ca.* −4.4 ppm (^{31}P) and ~5.0 ppm (^1H).

Table 1. H3′ and ^{31}P Chemical shifts (ppm) and H3′ H-P coupling constants (Hz) for P(en){d(ATGGGTACCCAT)} (12-mer) and Pt(en){d(TATGGGTACCCATA)} (14-mer)

	Coupling constants*		^{1}H Chemical shift†		^{31}P Chemical shift‡	
H3′	12-mer	14-mer	12-mer	14-mer	12-mer	14-mer
T_1		6.6		4.66		−4.17
A_2	5.5	3.3	4.90	5.03	§	−4.57
T_3	5.6	5.0	4.93	4.91	−3.67	−3.78
G_4	3.6	3.4	5.11	5.12	§	−4.14
G_5	<1.0	<1.0	4.83	4.84	−2.83	−3.00
G_6	5.1	4.7	4.8‖	4.8‖	−3.55	−3.85
T_7	4.8	5.2	4.71	4.71	−4.67	−4.64
A_8	6.8	6.9	5.05	5.05	−2.45	−2.65
C_9	8.0	8.2	4.84	4.83	§	−4.23
C_{10}	5.4	4.9	4.84	4.84	§	−4.40
C_{11}	5.3	5.1	4.87	4.88	§	−4.34
A_{12}	4.8	3.7	5.01	5.02	§	−4.40
T_{13}		5.3	4.5‖	4.81	§	−4.14
A_{14}				4.7‖		−4.17

* Values obtained from 2D *J* coupling experiment at 40°. Estimated accuracy of ±0.15 Hz.
† Values obtained from ^{31}P–^{1}H SRCSC experiment at 40° except where indicated.
‡ 12-mer at 25°, 14-mer at 40°.
§ ^{31}P shifts between −4.0 and −4.5 ppm.
‖ Approximate value.

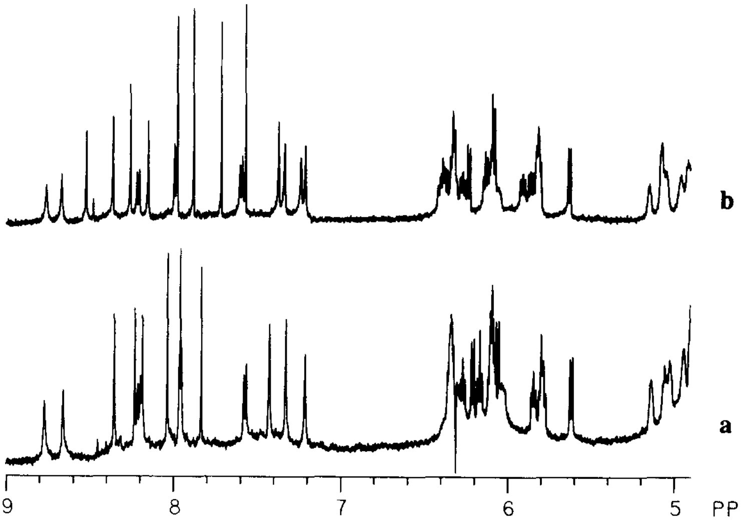

Fig. 3. The 500 MHz ^{1}H NMR spectrum of (a) Pt(en){d(ATGGGTACCCAT)} (0.025 M, 10^{-4} M EDTA, pH 7) and (b) Pt(en){d(TATGGGTACCCATA)} (0.030 M, 10^{-4} M EDTA, pH 7) at 22°.

six H8 signals present, it is established that one of these is the missing signal.

Since many crosspeaks are missing in comparison to B-form DNA, we chose to gain an entry into specific ^{1}H NMR assignments by several routes. Points of entry include: (a) HMQC and SRCSC ^{31}P–^{1}H correlation spectroscopies; (b) single frequency ^{31}P decoupling; and (c) the assumption that the ends were duplexed in a right-handed helix allowing limited use of standard internucleotide NOEs. Several of these approaches were combined to present a consistent picture of the assignments.

The more specific ^{1}H NMR assignments were initiated by use of ^{17}O-labeling based on ^{31}P assignments of the 14-mer combined with the HMQC ^{31}P–^{1}H correlation experiment [4] (Fig. 1). The region containing the H5′/5″ signals is crowded, so assignments using the ^{31}P–H3′ connectivities were employed. This signal is coupled to an H3′ at 5.04 ppm, assigning it as A_8. This result is also found in an SRCSC experiment (not shown). This A_8 H3′ has a moderately strong NOE crosspeak to the broad downfield signal at 8.67 ppm. This H3′ also has COSY connectivities through H2′/2″ protons to an H1′ signal at 6.07 ppm that has a NOE connectivity to the same downfield 8.67 ppm signal. On the basis of these results, the signal at 8.67 ppm is assigned as A_8 H8 and the H1′ is assigned as A_8 H1′. The ^{31}P NMR

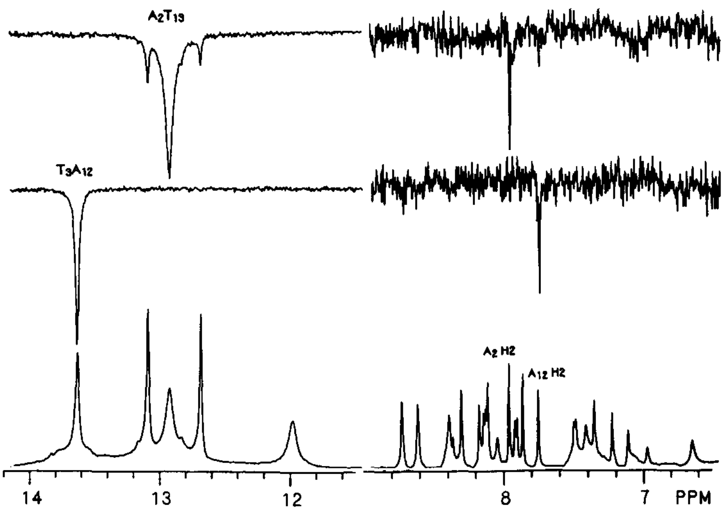

Fig. 4. One-dimensional NOE experiments with a solution of Pt(en){d(ATGGGTACCCAT)} (0.025 M, 10^{-4} M EDTA, pH 6.1, 10°, 10% D_2O). Shown are (bottom) the off-resonance irradiated reference spectrum, and the NOE difference spectra with irradiation imino signals of (middle) T_3A_{12}, and (top) A_2T_{13}.

signals assigned to T_3pG_4 and T_7pA_8 by analogy above have HMQC crosspeaks to H3′ signals with NOE crosspeaks to T H6 resonances. Using this method, the T_3 and T_7 H6 signals were assigned. These H6 signals have characteristics (e.g. crosspeak to G_4 H1′ and broadening at low temperature respectively) similar to those in the 14-mer where the ^{17}O assignments were performed. The remaining T H6 could then be assigned to T_{13}.

In this way, we were able to assign three of the six H3′ signals resolved between 4.65 and 5.20 ppm to T_3, T_7, and A_8. The most downfield of these six resolved H3′ signals at 5.13 ppm has a NOE crosspeak to an H8 signal assigned to G4 (see below). The signal at 5.01 ppm has a NOE crosspeak with an H8 signal at 8.38 ppm. This signal has a NOE crosspeak to a T methyl signal that is assigned to T_{13}. Therefore, the H3′ and H8 signals are assigned to A12. Similarly, the remaining resolved signal at 4.89 ppm clearly is for A_2 H3′ because of a NOE crosspeak to A_2 H8 assigned in the same manner as A_{12} H8. There are five remaining H3′ signals in the region, the three Cs, G_5, and G_6. These occur at *ca.* 4.8 ppm and overlap severely. The H3′ for T_{13} is observed at 4.53 ppm by its NOE crosspeak to T_{13} H6.

Although HMQC provided useful information, a limitation encountered in this experiment was that no scalar connectivities were observed with the G_5pG_6 and G_4pG_5 ^{31}P signals at 21°. The G_6pT_7 signal has a clear connectivity but to the severely overlapped H3′ signal.

Given the observation that the overlapping signal at 4.8 ppm contains the three C and two G H3′ signals, the following arguments assign the H3′ signals to G_6 and G_6. The HMQC experiment identifies one of these H3′ to be that for G_6. A selective irradiation (decoupling of the ^{31}P signal at −2.8 ppm assigned to G_5pG_6 by ^{17}O-labeling) demonstrates that the G_5 H3′ is also in this region. Therefore, the H3′ at 5.13 ppm is assigned to G_4, in agreement with the NOESY results (see below). The G_4 H8 is assigned to the signal at 8.18 ppm both by analogy to the 14-mer where the SRCSC experiment allows the H3′ assignment and by a NOE crosspeak to T_3H1′. The upfield position and sharpness of this signal strongly suggest that G_4 does not bind Pt. Assuming the aromatic proton signal assignments are correct thus far, it remains that the broad, most downfield H8 signal is for either G_5 or G_6. Its strong NOE crosspeak to the other broad downfield H8 signal, A_8, is characteristic of H8 signals of Pt crosslinked species [1–3, 13, 16]. These signals in the 14-mer undergo exchange in D_2O, identifying them as H8 signals. A summary of assignments is listed in Table 2.

(b) C H6, C H5. The C H6 assignments for Pt(en){d(ATGGGTACCCAT)} were made by analogy with the assignments for the 14-mer (see below). The H6 doublets come at very similar chemical shifts for the two oligomers. Independent assignments were not possible for the 12-mer due to a lack of a C_{11} H1′-A_{12} H8 NOE crosspeak. This crosspeak was observed for the 14-mer, and the H6 signal at 7.57 ppm is readily assigned to C_{11}. The NOE crosspeak observed between the C_{10} H1′ and C_{11} H6 for the 14-mer was also observed for the 12-mer. A weak connectivity between C_{10} H6 and C_{11} H5 was found for the 12-mer. The only remaining C H6 doublet must be the C_9 H6 signal. The C H6 and C H5 assignments are listed in Table 2.

(c) H1′. The most downfield H8 signal has been identified as either G_5 or G_6. Since the H8 signal of this nucleotide has only one NOE, i.e. a strong one to its H1′, it probably has the unusual *syn* conformation, hence the designation G_s. Of the remaining eleven H1′ signals, six have NOE crosspeaks to assigned A H8 or assigned T H6 signals. Two have

Table 2. Assignments of non-labile ^{1}H NMR signals (ppm) of Pt(en){d(ATGGGTACCCAT)}*

Base	H8/H6	H2/H5	H1′	H2′	H2″	H3′	H4′
A_2	8.23	8.02	6.26	2.71	2.88	4.89	4.28
T_3	7.42		5.74	2.23	2.52	4.94	4.25
G_4	8.18		6.08	†	2.89	5.13	4.47
G_m	‡		5.82	1.32	2.48	4.8§	4.04
G_s	8.75		6.30	2.68	3.38	4.8§	†
T_7	7.20		6.01	†	†	4.71	4.09
A_8	8.67	7.95	6.07	2.78	3.12	5.04	4.23
C_9	7.95	6.04	6.33	2.27	2.68	4.82	4.51
C_{10}	8.20	6.18	6.08	2.42	2.65	4.82	4.36
C_{11}	7.57	5.60	5.77	2.01	2.41	4.87	4.21
A_{12}	8.38	7.81	6.33	2.78	2.90	5.01	4.42
T_{13}	7.30		6.14	2.18	2.18	4.53	4.04

* Chemical shift values at 12° are listed.

† Unable to assign this signal.

‡ Signal is missing from spectrum.

§ G_6H3′ signal is at 4.80 ppm and G_5 H3′ signal is at *ca.* 4.8 ppm. Due to the unknown identity of G_m and G_s, both H3′ signals are listed at 4.8 ppm.

NOE crosspeaks to assigned C H6s. These two and a third C H6 signal have NOE crosspeaks to H3′ signals, which have COSY connectivities to H1′ signals. Thus, the nine H1′ signals for the three As, three Ts and three Cs are identified. The G_4 H8 has a crosspeak to an H1′ in addition to the H3′ signal discussed above. Therefore, the H1′ at 5.82 ppm which has no crosspeaks to an aromatic signal is assigned to G_m. Assignments are listed in Table 2. The following H8/H6 signals exhibited NOEs to the H1′ signal of the 5′ residue: T_3, C_{11}, and T_{13}. The G_s and T_7 H1′ signals are particularly broad.

The H1′ of G_m has a crosspeak to a signal in the H4′/5′/5″ region (most probably the H4′ of its own sugar). This signal has a weak crosspeak to the T_7 methyl signal. The H6 and H3′ signals of this T_7 have crosspeaks to the H1′ of G_s. In turn, the H2′/2″ signal of this deoxyribose has a weak crosspeak to the T_7 methyl. Therefore, there are crosspeaks between T_7 and signals of *both* unusual G moieties, G_s and G_m. Although G_s H8 has a strong NOE crosspeak to A_8 H8, this information is not enough to assign G_s to G_5 or G_6.

(d) A H2, NH. The assignments of the imino proton signals of Pt(en){d(ATGGGTACCCAT)} are based on the assumption of a stem region containing typical Watson–Crick base pairing [15, 17]. At 10° and pH 6.1, three sharp signals (13.64, 12.68, and 13.09 ppm), two moderately broad signals (12.93 and 11.98 ppm), and one very broad signal (~11 ppm) were observed. The sharp signal at 13.64 ppm occurs in the region where T N3 protons of AT base pairs are typically observed (15.0 to ~13.0 ppm) [24] and is assigned to the most internal AT base pair of the stem region, T_3A_{12}. The moderately broad signal at 12.93 ppm shifted downfield and sharpened upon temperature decrease, thus identifying it as the terminal AT base pair, A_2T_{13}. The sharp signal at 12.68 ppm occurs in the region where G N1 protons of GC base pairs are usually observed (~13.0 to 12.0 ppm) [24]. The sharp signal at 13.09 ppm occurs in an intermediate range. The upfield positions of the signals at 11.98 and ~11 ppm suggest weak and very little H-bonding respectively.

1D NOE experiments were conducted on a water solution of Pt(en){d(ATGGGTACCCAT)} at pH 6.1 and at 5° and 10°. The experiments at 10° (Fig. 4) are described for reasons discussed above, but similar results were obtained at 5°. Strong NOEs are characteristically observed between the T N3 proton of an AT base pair in duplexed DNA and the A H2 proton within that base pair [23]. Irradiation of the signal assigned as A_2T_{13} (12.93 ppm) resulted in the observation of an NOE for the A H2 signal at 7.95 ppm, thus identifying it as A_2 H2 (Fig. 4). A similar NOE was observed between the T_3A_{12} imino signal at 13.64 ppm and the A_{12} H2 at 7.75 ppm (Fig. 4). By difference, the A H2 at 7.85 ppm was assigned as A_8. No evidence for a base pair between A_8 and T_7 was found.

Hydrogen bonded NH (NH_a) of C residues within GC base pairs are 2.5 Å from the G N1 proton [23], and the signal usually occur in the region between 8 and 9 ppm [25]. The signal of the non-hydrogen bonded C NH (NH_b) typically is observed further upfield (7 to 6.5 ppm) [25]. The C H5 is only 2.4 Å from the NH_b [23]. Irradiation of the probable GC signal at 12.68 ppm produced a medium NOE to a NH signal at 8.37 ppm. The downfield position of this NH signal identifies it as the NH_a of the C within the GC base pair. Irradiation of this signal resulted in a strong NOE to another NH signal at 6.96 ppm, identifying it as the NH_b of the same C. Irradiation of C_{11} H5 resulted in an NOE at this NH_b. Therefore, the imino signal at 12.68 ppm is assigned as G_4C_{11} and the signals at 8.37 and 6.96 ppm as C_{11} NH_a and C_{11} NH_b respectively. The G_5C_{10} imino signal at 13.09 ppm and the C_{10} NH_2 signals at 8.00 and 7.38 ppm are identified in the same manner. Irradiation of the G_5C_{10} imino signal also resulted in weak NOEs at A_8 H2 and C_{11} NH_a. The broad signal at 11.98 ppm had no NOE to any other signal. No evidence for a G_6C_9 base pair was found. These results strongly suggest that base pairing occurs between the section containing A_2 through G_5 and the section containing C_{10} through T_{13}. No base pairing is indicated in the region between G_6 and C_9. However, we cannot rule out the possibility that G_6 rather than G_5 is base paired with C_{10}. Weak interimino NOEs were also observed between T_3A_{12} and G_4C_{11}, and between G_4C_{11} and G_5C_{10}. No NOE was observed between A_2 T_{13} and T_3A_{12} imino signals possibly due to duplex fraying at the terminal base pair and the broadness of the A_2T_{13} imino signal.

Other NOE results obtained in a set of experiments at 5° are of interest. Irradiation of C_{11} NH_a resulted in a NOE at A_8 H2. A very weak NOE is observed from T_7 Me to the broad downfield G_s H8. NOEs were observed to the G_4C_{11} imino proton from the C_9 H6 (medium), the broad downfield G_s H8 (weak), and the H1′ of G_m (weak). Irradiation of A_8 H8 resulted in a weak NOE at G_5C_{10}. These NOE results are particularly interesting since they indicate that protons on remote bases (or sugars) are in proximity.

(e) H2′/H2″. Assignments of H2′H2″ signals were made via a combination of NOESY and COSY results (Table 2). H2″ signals are typically observed downfield of H2′ signals [26]. Therefore, the more downfield signal of each H2′/H2″ pair is designated H2″. Each H8/H6 signal, except for G_s H8 and T_7 H6, exhibited a NOE crosspeak to its own H2′ and/or H2″. H2′-H2″ and H2′/H2″-H1′ COSY connectivities then enabled further identifications. For example, the H2′/H2″ signals of G_s were assigned on the basis of a G_s H1′-H2″ COSY connectivity and a subsequent G_s H2″-H2′ crosspeak. The G_s H2″ is unusually far downfield (3.38 ppm). T_7 H6, H1′, and H3′ do not exhibit a NOE or COSY crosspeak to any H2′/H2″, thereby preventing the assignment of T_7 H2′/H2″. It is worth noting that at 12°, T_7 H6 is slightly broad and T_7 H1′ is very broad. The H2′/H2″ signals of G_m are identified at 2.48 and 1.32 ppm. The 1.32 ppm signal is unusually far upfield. The following H8/H6 signals exhibit a NOE to the H2″ signal of the 5′ residue: T_3, G_4, A_{12}, and T_{13}.

(f) H4′. Seven H4′ signals (A_2, T_3, G_4, C_{10}, C_{11}, A_{12}, T_{13}) were assigned on the basis of COSY connectivities to assigned H3′ signals (Table 2). These assignments were confirmed by intranucleotide NOE crosspeaks with H8/H6 and H1′ signals. T_7, A_8, C_9, and G_m H4′ signals were assigned on the basis of H1′ NOE crosspeaks. A_8 H8 and C_{10} H6 signals exhibited NOEs to their own H4′ signals and to the H4′ signals of the 5′ residue. C_9 H6 has only one NOE in this region and that was to A_8 H4′. Internucleotide NOEs between H8/H6 signals and H4′ signals of the 5′-residue are not typically observed for duplexed DNA [23].

H3′-P *Coupling constants*. The heteronuclear 2D *J* coupling experiment permits measurement of ${}^3J_{HCOP}$ coupling constants for each base H3′ (Table 1). Many of the coupling constants listed are significantly greater or less than those observed for typical duplexed DNA and oligodeoxyribonucleotides (3–5 Hz) [20], indicating distortions in the phosphate backbone. A Karplus relationship correlating ${}^3J_{HCOP}$ with the H-C-O-P dihedral angle has been proposed [27]:

$$J_{HCOP} = 15.3 \cos^2 \phi - 6.1 \cos \phi + 1.6$$

This equation is a multi-varied function, resulting in four possible ϕ values for any given *J*. Since the platinated oligonucleotides Pt(en){d(TATGGGTACCCATA)} and Pt(en){d(ATGGGTACCCAT)} have unusual structures and we do not, at this point, have a definite model of these structures, none of these calculated ϕ values can be discarded. However, the ϕ values calculated for each phosphate group are valuable as contraints in any future molecular mechanics calculations, especially since there is a deficiency of internucleotide NOEs in this system. It is of interest that the most atypical values are those for G_5 (not observed and therefore probably less than 1 Hz), A_8 (6.8 Hz), and C_9 (8.0 Hz), all bases within the loop of the proposed hairpin-like structure.

pH Dependence. Since only fourteen of the fifteen nonexchangeable base protons of Pt(en){d(ATGGGTACCCAT)} were observed, the pH dependence of these signals was investigated (Fig. 5). Unfortunately, at pH >10.6 and <4.1, many of the signals broadened substantially and could no longer be followed. However, from pH 7.90 to 10.53, an upfield shift (~0.3 ppm) was observed for the most downfield G H8 signal. This behavior resembles that of other G H8 signals of [d(GG)-N7,N7]*cis*Pt(amine)$_2$ moieties [4, 7]. The A_8 H8 signal shifted only slightly downfield in this pH range. This signal, however, did shift ~0.2 ppm downfield as the pH decreased from 7.04 to 4.18.

For *cis*Pt(NH$_3$)$_2${d(TCTCGGTCTC)-N7(5), N7(6)}, den Hartog *et al.* [7] observed a significant upfield shift between pH 8 and 10 of the T H6 signal for the T residue immediately 3′ to the Pt binding site. This result was attributed to an effect from the N1 deprotonation of the neighboring G (also undergoes an upfield shift). As mentioned above, we observed the upfield shift of a platinated G H8. However, there was little change in T_7 H6 (or any other T H6) between pH 8 and 10. This would seem to indicate that T_7 is not immediately 3′ to G_s, and therefore G_s is assigned as G_5. However, because of the unusual structure of this oligomer, this assignment can be only tentative.

C_{10} H6 shifted upfield (~0.04 ppm) from pH 7.90 to 10.24. Above pH 10.24, it broadened beyond observation. The other two C H6 signals shifted only slightly in this pH range and were observable at pH 10.53. As the pH was lowered from 7.04 to 4.18, C_9 H6 shifted ~0.2 ppm downfield. Only small shifts were observed for C_{10} and C_{11} H6 in this range.

In the low pH range (7.04 to 4.18), the three A H2 signals behaved similarly to one another, i.e. they shifted slightly downfield. In the high pH range (7.04 to 10.53), the A H2 signals exhibited differing behaviors. A_{12} H2 shifted slightly downfield, A_8 H2 shifted slightly upfield, and A_2 H2 did not shift. The A_2, A_{12}, and G_4 H8 signals exhibited few changes in chemical shift between pH 4.18 and 10.53

KCN addition. Two samples of Pt(en){d(ATGGGTACCCAT)} (pH 7.0), one in D_2O and one in H_2O, were treated with KCN to remove the Pt moiety from the oligonucleotide. The pH changed to 10.3 immediately after KCN addition and

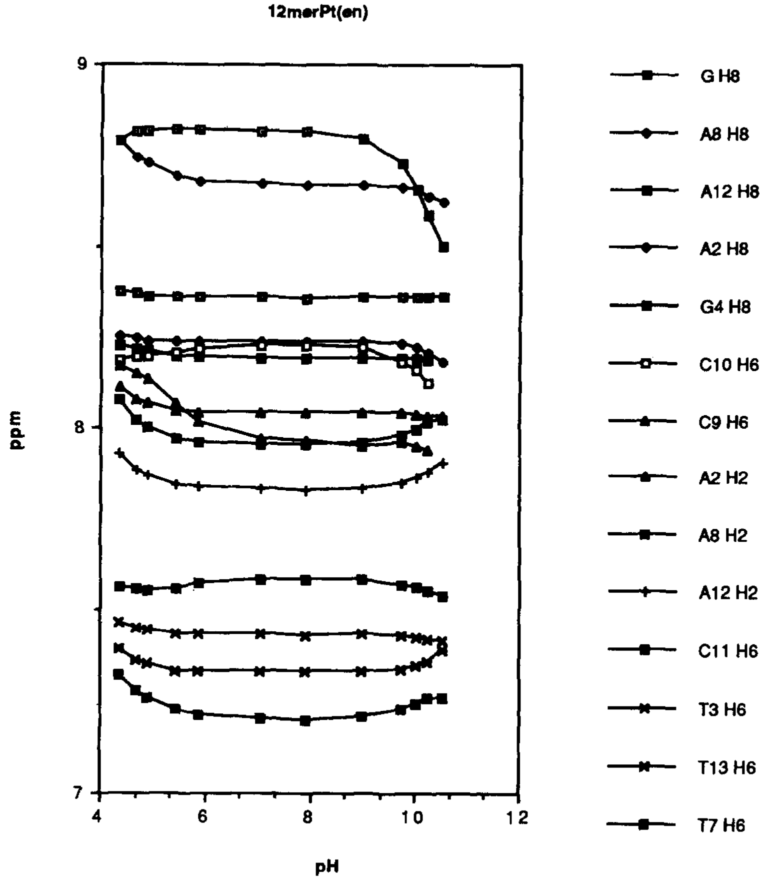

Fig. 5. The pH dependence of the ^1H NMR signals (9.0 to 7.0 ppm region) of Pt(en){d(ATGGGTACCCAT)} (0.015 M, 10^{-4} M EDTA, 22°) in D_2O.

remained constant. ^1H NMR spectroscopy indicated a total reaction time of *ca.* 60 hr. New signals appeared corresponding to those observed for the $d(ATGGGTACCCAT)_2$ duplex (see above) (Fig. 6). All 15 base signals were present in spectra recorded at pH 10.3 and 7.0.

Pt*(en){d(TATGGGTACCCATA)}* *(14-mer) Results*

^{31}P *NMR Spectroscopy.* The 14-mer ^{31}P NMR spectrum has been assigned by ^{17}O-labeling methods [15, 17]. Shifts are given in Table 1. In addition to 7 signals in the normal shift range of −3.9 to −4.4 ppm, the ^{31}P NMR spectrum of Pt(en){d(TATGGGTACCCATA)} (14-mer) exhibited two signals shifted considerably downfield (−2.57, −2.89 ppm), two signals slightly downfield (−3.67, −3.75 ppm), and two signals slightly upfield (−4.57, −4.70 ppm).

^1H *NMR Spectroscopy. 9 to 7 ppm Region.* The aromatic region of Pt(en){d(TATGGGTACCCATA)} consists of 17 signals, including two broad downfield signals (Fig. 3). Eighteen should be present.

15 *to* 10 *ppm Region.* The spectrum of a solution of Pt(en){d(TATGGGTACCCATA)} (0.03 M, pH 7.0, 5°) had sharp signals at 13.57, 13.53, 13.14, and 12.65 ppm with relative areas of 1 : 1 : 1 : 1. Two broad signals were observed at 12.0 and 11.1 ppm. Decreasing the pH to 6.0 caused the signal at *ca.* 12.0 ppm (pH 7.0) to sharpen and two signals were observed at 12.10 and 11.96 ppm. The broad signal at ~11.1 ppm also sharpened and shifted downfield slightly to ~11.0 ppm. No signals in this region were observed when the sample was dried and the spectrum recorded immediately after addition of D_2O at 5°.

Assignments. (a) H3′, T H6, A H8, G H8. 2D NOE and COSY experiments were conducted on Pt(en){d(TATGGGTACCCATA)} (pH 7.0, 0.030 M). The results obtained were very similar to those obtained for the 12-mer analogue (see above). The T H6, C H6, A H2, and H8 signals were characterized similarly.

Although the additional two nucleotide units in Pt(en){d(TATGGGTACCCATA)} compared to the 12-mer complicate the ^1H NMR assignments (Table 3), there is slightly less overlap in the ^{31}P spectrum of the 14-mer, possibly because of lower conformational flexibility of the larger oligomer due to the longer stem of the hairpin-like molecule. We decided to exploit this feature of the ^{31}P spectrum of Pt(en){d(TATGGGTACCCATA)} by using the ^{31}P–^1H SRCSC experiment [20] to aid in assigning the ^1H spectrum. Also, the complete assignment of the

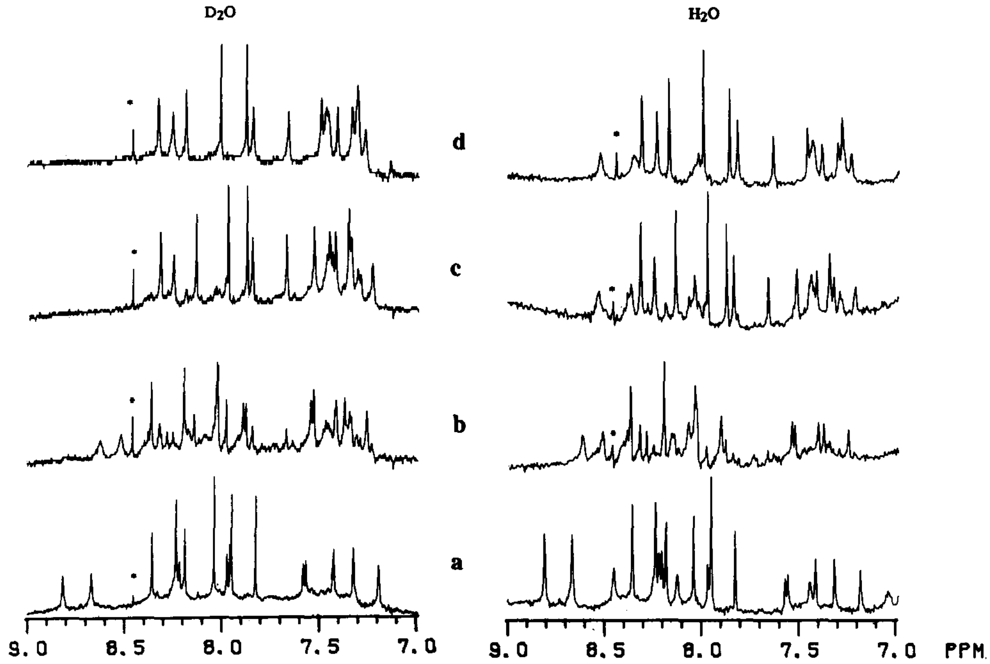

Fig. 6. The 500 MHz ^{1}H NMR spectra of Pt(en){d(ATGGGTACCCAT)} in D_2O and H_2O after addition of KCN. Shown are spectra at (a) t = 0 (before addition), pH 7.0; (b) t = 7 hr, pH 10.3; (c) t = 2 days, pH 10.3; and (d) t = 4 days, pH 7.0.

Table 3. Assignments of non-labile ^{1}H NMR signals (ppm) of Pt(en){d(TATGGGTACCCATA)}*

Base	H8/H6	H2/H5	H1′	H2′	H2″	H3′	H4′
T_1	7.38		5.81	1.83	2.24	4.70	4.04
A_2	8.54	7.85	6.40	2.92	3.06	5.08	4.49
T_3	7.34		5.78	2.20	2.55	4.95	4.20
G_4	8.15		6.07	2.88	†	5.12	4.48
G_m	‡		5.80	1.38	2.48	4.8§	4.00
G_s	8.74		6.31	2.72	3.37	4.8§	†
T_7	7.22		6.04	2.68	†	4.73	4.10
A_8	8.68	7.97	6.08	2.79	3.12	5.05	4.24
C_9	7.98	6.07	6.36	2.28	2.71	4.83	4.54
C_{10}	8.21	6.21	6.21	2.45	2.66	4.82	4.40
C_{11}	7.58	5.61	5.78	2.10	2.49	4.87	4.23
A_{12}	8.37	7.69	6.26	2.66	2.88	5.03	4.41
T_{13}	7.21		5.85	1.93	2.28	4.84	4.15
A_{14}	8.24	7.51	6.32	2.45	2.68	4.74	4.22

* Chemical shift values at 12° are listed.

† Unable to assign this signal.

‡ Signal is missing from spectrum.

§ G_6 H3′ signal is at 4.80 ppm and G_5 H3′ signal is at ~4.8 ppm. Because of the unknown identity of G_m and G_s, both H3′ signals are listed at 4.8 ppm.

^{31}P NMR signals for the 14-mer and the resolution of the crosspeaks in the SRCSC experiment (as compared to the HMQC experiment) allow more H3′ signals, both within the overlapping region at ~4.83 ppm and outside this region, to be assigned independently of NOE results. In particular, the G_4 H3′ signal can be unambiguously assigned. The SRCSC experiment on Pt(en){d(TATGGGTACCCATA)} was conducted at 12°, the temperature of the NOESY experiment, and the temperature at which more (twelve) ^{31}P–^{1}H crosspeaks could be resolved (Fig. 2A).

At 12°, the furthest downfield ^{31}P NMR signal at −2.6 ppm [corresponding to the peak folded over at ~−4.4 ppm (^{31}P) and ~5 ppm (^{1}H) in Fig. 2A], assigned as A_8pC_9 by ^{17}O-labeling, is coupled to an H3′ at 5.05 ppm. This H3′ has a NOE crosspeak to the broad downfield ^{1}H signal at 8.68 ppm (12°), thus assigning these two signals (H3′ and H8) as A_8. This method was used to assign the H3′ signals of A_2 and

T_7 at 5.08 and 4.73 ppm as well as their respective H8 and H6 signals (8.52 and 7.22 ppm) (12°). The two ^{31}P signals at −3.67 and −3.75 ppm (0.1 M $NaNO_3$, 25°) were assigned to G_6pT_7 and T_3pG_4, respectively [15, 17]. At 12° (no salt), these two signals are overlapped and only one ^{31}P–^1H crosspeak is observed.

At 40° (no salt), signals are observed at −3.78 and −3.85 ppm. The −3.78 ppm signal exhibits coupling to an H3′ at 4.93 ppm (40°) that has a NOE crosspeak to an unassigned T H6 at 7.34 ppm (12°). On this basis, these two proton signals (H3′ and H6) are assigned as T_3. The −3.85 ppm signal, which must then be G_6pT_7, exhibits a crosspeak to an H3′ at 4.80 ppm (within the overlapping region). At 12°, G6 H3′–^{31}P coupling is either not observed or the T_3 and G_6 H3′ signals are coincident. These results indicate that differing salt concentration leads to reversal in shift order of the two ^{31}P signals.

As for the 12-mer, a NOESY crosspeak was observed between the A_2 H8 and T_3 Me signals in the 14-mer. A similar crosspeak was observed between unassigned H8 and T Me signals, thus identifying them as A_{12} H8 and T_{13} Me. A COSY crosspeak to T_{13} Me assigns T_{13} H6. With the T_3, T_7, and T_{13} H6 signals assigned, the unassigned T H6 at 7.38 ppm must be T_1. T_1 H6 has a NOE crosspeak to a H3′ signal at 4.70 ppm (12°) which is coupled to a ^{31}P signal in the normal region.

A heteronuclear 2D *J* experiment [20] which yields the H3′-C-O-P coupling constants was conducted on Pt(en){d(TATGGGTACCCATA)} (Fig. 2B). It was necessary to conduct this experiment at 40° due to interference of the HDO signal at lower temperatures. Two H3′ signals exhibiting no observable coupling to ^{31}P were oberved at 4.71 and 4.84 ppm (40°). A_{14} has no 3′ phosphate group since it is at the 3′ end. The H3′ signal at 4.71 ppm is assigned to A_{14} for two reasons. First, the H3′ signal of the most 3′ base is generally found to occur upfield of most or all other H3′ signals [14]. Second, this H3′ has a NOE crosspeak to an H8 at 8.24 ppm (12°) assigned to A_{14} on the basis of a NOE to T_{13} H1′ (see below). The G_5pG_6 ^{31}P signal at −3.00 ppm (40°) exhibits <1 Hz coupling to an H3′. However, by analogy to the 12-mer, the weakly coupled H3′ in the overlapping region at ~4.83 ppm (40°) is assigned as G_5. The G_4 H8 at 8.15 ppm was assigned on the basis of a NOE to T_3 H1′ (see below). A NOE crosspeak to the H3′ at 5.12 ppm assigns this signal to G_4. The C H6 signal at 7.58 ppm has a NOE to the isolated H3′ at 4.87 ppm (12°). This H3′ is coupled to a normal region ^{31}P signal at −4.34 ppm (40°) which ^{17}O-labeling indicates is $C_{11}pA_{12}$. These two signals (H6 and H3′) are therefore assigned to C_{11}. ^{31}P NMR signals assigned by ^{17}O-labeling as C_9pC_{10} (−4.23 ppm, 40°) and $C_{10}pC_{11}$ (−4.40 ppm, 40°) have ^{31}P–^1H crosspeaks (12° and 40°) to two overlapping H3′ signals at 4.83 ppm. One C H6 (C_{10}, see below) has a NOE to a signal in this region. Thus, C_9H3′ and C_{10} H3′ are at *ca.* 4.83 ppm. The H3′ assignments made for the 14-mer by use of the SRCSC, 2D *J*, and NOESY experiments are fully consistent with those of the 12-mer (*vide supra*). As in the 12-mer, the assignments thus far identify the furthest downfield broad H8 signal as G_5 or G_6. A strong NOE is observed between this signal and A_8 H8.

(b) C H6, C H5. In a right-handed duplex, H8 signals typically exhibit a NOE crosspeak with the H1′ signal of its own sugar and of the sugar 5′ to it. 1D NOE results of Pt(en){d(TATGGGTACCCATA)} (see below) and of its 12-mer analogue (see above) strongly indicate that base pairing exists in the region between C_{10} and A_{12}. The assignment of C_{11} H6 above is confirmed by the observation of a NOE crosspeak between the A_{12} H8 and the C_{11} H1′ signal at 5.78 ppm. C_{11} H6 has a NOE crosspeak to the H1′ signal (6.12 ppm) assigning it to C_{10} H6. The NOE crosspeak for the C H6 at 8.21 ppm assigns it as C_{10}. The remaining C H6 at 7.98 ppm is assigned as C_9. By NOESY and COSY connectivities, the C H5 signals are assigned (Table 3).

(c) H1′. Each H8/H6 signal has a NOE crosspeak to the H1′ signal of its own sugar, thus leading to the assignments listed in Table 3. G_4 H8 and A_{14} H8 were assigned on the basis of NOEs to H1′ signals of T_3 and T_{13} respectively. The following H8 and H6 signals also exhibit crosspeaks to the H1′ signal of the sugar in the 5′ direction: T_3 H6-A_2 H1′, G_4 H8-T_3 H1′, C_{11} H6-C_{10} H1′, A_{12} H8-C_{11} H1′, T_{13} H6-A_{12} H1′, and A_{14} H8-T-13 H1′. This pattern is typical for a DNA duplex [23] and is not observed for residues G_5 through C_{10}. As in the 12-mer analogue, the most downfield H8 (G_5 or G_6) has only two NOEs and one is a strong one to its H1′.

(d) A H2, NH. At 5° and pH 6.1, four sharp signals (13.53, 13.46, 13.10, and 12.62 ppm), two moderately broad signals (12.05 and 11.95 ppm) and a very broad signal at *ca.* 11 ppm were observed. The signal at 11.95 ppm shifted upfield and broadened upon raising the temperature to 10°. At 1°, this signal is coincident with the 12.05 ppm signal. This behavior suggests the assignment of this signal (11.95 ppm) as the terminal T_1A_{14}. The next signal to be affected by an increase in temperature is that at 13.46 ppm (5°). Increasing the temperature to 22° shifted this signal to 13.36 ppm and broadened it, identifying it as A_2T_{13}. The remaining signal in the AT imino proton region must be T_3A_{12}.

1D NOE experiments were conducted on a water solution of Pt(en){d(TATGGGTACCCATA)} at pH 6.1 and 1°. Irradiation of the A_2T_{13} and T_3A_{12} signals resulted in strong NOEs at 7.78 and 7.62 ppm, respectively, assigning them as A_2 H2 and A_{12} H2. At 1°, irradiation at 12.05 ppm produced an NOE at 7.43 ppm. This result is complicated by the presence of two signals at 12.05 ppm, T_1A_{14} and an unidentified signal. However, an NOE is typically observed between the T N3 proton of a AT base pair and the A H2 proton within that base pair [23]. One signal at 12.05 ppm is, therefore, assigned as T_1A_{14} and the A H2 at 7.43 ppm is A_{14}. By difference, the signal at 7.89 ppm must be A_8 H2. The G_4C_{11} and G_5C_{10} imino proton signals at 12.62 and 13.10 ppm, respectively, are assigned by methods described for Pt(en){d(ATGGGTACCCAT)} (see above). Weak inter-imino NOEs were also observed between the following base pairs: A_2T_{13}, T_3A_{12}; T_3A_{12}, G_4C_{11}; and G_4C_{11}, G_5C_{10}.

(e) H2′/H2″. All assignments listed in Table 3 were made on the basis of COSY connectivities with assigned H1′ signals and with each other except for A_{14} H2′ (NOE to A_{14} H8) and T_7 H2′ (COSY connectivity with T_7 H3′). As with the 12-mer, the G_m H2″ is unusually far upfield (1.38 ppm) and G_s H2′ is unusually far downfield (3.37 ppm). The following H8/H6 signals exhibit a NOE to the H2′ of the 5′ residue: T_3, G_4, A_{12}, T_{13}, and A_{14}.

(f) H4′. Nine H4′ signals (T_1, A_2, T_3, G_4, C_{10}, C_{11}, A_{12}, T_{13}, and A_{14}) were assigned on the basis of COSY connectivities to assigned H3′ signals (Table 3). These assignments were confirmed by NOE crosspeaks with H8/H6 and H1′ signals. T_7, A_8, C_9, and G_m H4′ signals were assigned on the basis of H1′NOE crosspeaks. A_8 and C_{10} H6 signals exhibited NOEs to their own H4′ and to the H4′ signals of the 5′ residue. C_9 H6 had only one NOE in this region and that was to A_8 H4′. No crosspeaks were evident between G_s H8 or H1′ and any H4′ signals.

H3′-P *Coupling constants.* Coupling constants between ^{31}P and H3′ nuclei were measured via the 2D J coupling experiment (Fig. 2B). Table 1 contains the $^3J_{HCOP}$ coupling constants measured for each base H3′. The values measured for the 14-mer are consistent with those measured for the 12-mer, the only differing values being for the residues at the end of the stem region.

KCN addition. A sample of Pt(en){d(TATGGGTACCCATA)} was treated with KCN to remove the Pt moiety from the oligonucleotide. The reaction was monitored by ^1H NMR spectroscopy and electrophoresis. The stripped oligomer was purified by HPLC methods and digest analysis produced a ratio of 4A:4T:3G:3C.

^{195}Pt *NMR Spectroscopy*

The ^{195}Pt NMR spectrum of solutions of Pt(en){d(ATGGGTACCCAT)} and Pt(en){d(TATGGGTACCCATA)} revealed signals at −2645 and −2640 ppm respectively. These chemical shifts are similar to the reported shift for $[Pt(en)(Guo)_2]^{2+}$ (−2662 ppm) in which Pt is bound to two purine bases via N7 [28]. This similarity strongly suggests that the Pt in both species is bound to two purine bases via N7 and that the immediate environment of the Pt moiety is not greatly different from that in the model [28, 29].

UV Spectroscopy

The melting behavior of Pt(en){d(ATGGGTACCCAT)} as monitored by UV absorbance was similar to that observed for the platinated 14-mer and 10-mer oligomers, i.e. a featureless rise in absorbance from 15° to 75° [15, 17].

Electrophoresis

The electrophoretic characteristics of $d(ATGGGTACCCAT)_2$ and Pt(en){d(ATGGGTACCCAT)} were similar to those exhibited for the 14-mer and 10-mer oligomers [15, 17].

DISCUSSION

We have examined the nature of the hairpin-like structure formed by Pt anti-cancer drugs and self-complementary oligonucleotides $d(TATGGGTACCCATA)_2$ and the shorter 12-mer and 10-mer analogues. The similarity of the ^{31}P NMR spectra of the three oligomers allowed us to assign the unusually shifted ^{31}P NMR signals of the 12-mer by analogy to the assigned signals of the 14-mer and the 10-mer. With ^1H NMR spectra recorded at 500 MHz (Fig. 3), we have confirmed the absence of one aromatic signal as deduced earlier at 360 MHz. Therefore, the missing signal is probably not due to overlap. The ^1H assignments obtained by 2D NMR techniques (Tables 2 and 3) confirm the existence of a hairpin-like structure and provide further information on that structure.

For both the 14-mer and the 12-mer, our evidence suggests that a stem region exists involving terminal AT base pairing, G_4C_{11}, and probably G_5C_{10}. The phosphate groups T_1pC_2, G_4pG_5, and all phosphate groups in the 3′ direction of C_9 give rise to ^{31}P signals within the normal range. A_2pT_3 and T_3pG_4 exhibit ^{31}P signals only slightly outside the normal range. Also, $^3J_{H3'\text{-}P}$ values for H3′ signals of T_1, A_2, T_3, G_4, C_{10}, C_{11}, A_{12}, and T_{13} (Table 1), were within the range (3–6 Hz) usually observed for a DNA duplex. Typically, $^3J_{H3'\text{-}P}$ values for single strands are higher (5–7 Hz) [30]. Values as low as those observed for A_2 [3.3 Hz (14-mer)], G_4 [3.6 Hz (12-mer), 3.4 Hz (14-mer)], and A_{12} [3.7 Hz (14-mer)] are typical for double-stranded DNA [20] but not for single-stranded DNA. Gorenstein *et al.* [31] have observed a correlation of an upfield shift of ^{31}P signals and a decrease in $^3J_{H3'\text{-}P}$ for duplexes. For A_2P and $A_{12}p$, a similar correlation (upfield ^{31}P shift and $^3J_{H3'\text{-}P}$ decrease) occurs upon addition of the residues T_1 and A_{14}. Therefore, the sugar phosphate backbone of the stem appears normal.

^1H NMR results also suggest a right-handed duplex structure for the stem region. For the 12-mer, only four typical imino signals are observed between 15 and 12 ppm (Fig. 4), whereas six would be expected for a complete duplex structure for the oligomer. For the 14-mer, five typical imino signals are observed [15]. In 1D NOE experiments for Pt(en){d(ATGGGTACCCAT)}, strong NOEs were observed between two imino signals (12.98 and 13.68 ppm) and two A H2 signals (7.93 and 7.72 ppm) respectively (Fig. 4). NOEs are characteristically observed between the T N3 proton of an AT base pair in duplexed DNA and the A H2 proton within that base pair [23]. The 13.68 ppm signal is broad and exhibits temperature behavior typical for a terminal base pair. The 12.98 ppm signal occurs in the AT imino signal region for typical DNA duplexes [24]. These results are consistent with the existence of normal Watson–Crick A_2T_{13} and T_3A_{12} base pairs. Similar results were obtained for the 14-mer. The 1D NOE studies also suggested that G_4C_{11} and G_5C_{10} form base pairs. In a series of experiments, NOEs were exhibited from the assigned C_{10} and C_{11} H5 signals through their respective C NH_a and C NH_b signals to the imino signals observed at 13.08 and 12.68 ppm respectively. The presence of weak inter-imino NOEs supports the existence of a stem region with typical base pair stacking.

For right-handed duplex DNA, certain internucleotide NOEs are characteristic [23], particularly between H8/H6 protons and sugar protons (H1′, H3′, H2′/H2″) of the 5′ nucleotide. In 2D-NOE studies of Pt(en){d(ATGGGTACCCAT)} and Pt(en){d(TATGGGTACCCATA)}, many of these characteristic NOEs were observed for nucleotides within the stem region (T_1 through G_5 and C_{10} through A_{14}). For example, for the 14-mer, the H8/H6 signals of the following bases exhibited NOEs to the H1′, H2′, and H3′, signals of the 5′ residue: T_3, G_4, A_{12}, and T_{13}. Crosspeaks were also observed between A_2 H8 and T_1 H3′, between C_{11} H6 and C_{10} H1′, and between A_{14} H8 and T_{13} H1′, H2′.

Additional evidence for a normal stem was obtained in the ^{1}H signal pH dependence study of the 12-mer (Fig. 5). All aromatic signals for nucleotides within the stem region exhibited typical pH behavior [14]. No chemical shift changes are expected for H8 signals between pH 4 and 10, and none were observed for the A_2, G_4, and A_{12} H8 signals. From pH 9 to 10.4, T_{13} H6 shifts slightly downfield, indicating deshielding as a result of decrease in base stacking at the end of the stem region. T_3 H6 does not exhibit this behavior.

In contrast to this typical set of characteristics for the stem, NMR studies indicate a distorted sugar-phosphate backbone for the loop region $G_5pG_6pT_7pA_8pC_9$. The ^{31}P signals of G_5pG_6 and A_8pC_9 are far downfield of the normal range (*ca.* −2.9 and −2.6 ppm respectively). G_6pT_7 and T_7pA_8 give rise to ^{31}P signals slightly downfield and slightly upfield of the normal range respectively. $^3J_{H3'-P}$ coupling constants measured for several H3′ signals in this region are unusual (Table 1). $^3J_{H3'-P}$ for C_9p [8.0 Hz (12-mer), 8.2 Hz (14-mer)] is significantly higher than values measured even for single strands [30]. No H3′-P coupling was observed for G_5 at 40°.

For *cis*Pt(NH_3)$_2${d($T_1C_2T_3C_4G_5G_6T_7C_8T_9C_{10}$)-N7(5),N7(6)}, also an oligomer with a distorted structure, a similar result was obtained [2, 3]. At 32°, the H3′-P coupling of G_5 of this oligomer was not observable in a 2D *J* experiment. At 40°, a coupling constant of 8.9 Hz was measured, but the intensity of the signal was very low. Raising the temperature further to 48° decreased the coupling constant to 8.5 Hz and increased the signal intensity. Thus, as the distorted structure was disrupted, the conformation of the Gp moiety changed and the H3′-P coupling became more observable. A similar situation may exist with the 14-mer and the 12-mer. The lack of an intranucleotide H4′-H1′ NOE suggests that the conformation of the G_5 sugar is changed significantly upon platination, resulting in smaller $^3J_{H3'-P}$ values and cancellation of antiphase components in the 2D NMR experiments. The lack of observable coupling even at 40° may be due to the greater stability of the 12-mer and the 14-mer compared to *cis*Pt(NH_3)$_2${d(TCTCGGTCTC)-N7(5), N7(6)} [2, 3, 15, 17].

^{1}H NMR results are also consistent with a loop structure for the region $G_6T_7A_8C_9$. 1D NOE studies strongly indicate that no base pairing occurs in this region. Irradiation of the two upfield imino signals does not give any NOEs. 2D NMR experiments revealed behavior uncharacteristic of duplex DNA for nucleotides in the loop region. First, many COSY connectivities between sugar protons of these nucleotides are missing. The distorted structure probably changes the sugar conformations, resulting in different ^{1}H–^{1}H coupling constants. Second, many internucleotide NOEs typically observed for duplexed DNA are not exhibited for these nucleotides. Unlike the stem region, no NOEs are observed between the T_7 H6, A_8 H8, and C_9 H6 signals and the H1′, H2′/H2″, or H3′ signals of the respective 5′ residues. However, A_8 H8, C_9 H6, and C_{10} H6 each exhibited NOEs to the H4′ signal of the 5′ residue, a result not observed for protons in the stem region. This type of internucleotide NOE is not typical for right-handed helices, but is observed for Z-DNA [32].

Due to its unusual nature, the structure of the loop region is of particular interest. There does not seem to be any uniform configuration in this region; each nucleotide is unique. ^{31}P NMR results do not suggest a very unusual structure for the phosphodiester bonds on either side of T_7. The slightly downfield and slightly upfield shifts of the 5′ and 3′ phosphate groups, respectively, suggest small changes in bond or torsion angles. $^3J_{H3'-P}$ values are normal for each phosphate group, indicating no appreciable change in the C4′-C3′-O3′-P torsional angles.

^{1}H NMR results indicate that the T_7 base moiety is located within the space encircled by the loop. T_7 signals exhibit NOEs to signals of other nucleotides within the loop region. For the 12-mer, T_7 Me has NOEs to G_m H4′, G_s H8 and H2″, and C_9 H6 or A_8 H2 (overlap at 7.98 ppm). T_7 H6 and H3′ signals each have a NOE to G_s H1′. This type of result is also found with hairpins, e.g. for a $T_aT_bT_cT_d$ loop, T_c Me has NOEs to the H1′ signals of T_a, T_b, and T_c [33]. In the pH dependence study of Pt(en){d(ATGGGTACCCAT)} (Fig. 5), the T_7 H6 signal exhibits behavior similar to that of the other two T H6 signals, suggesting that the T_7 base stacks and is weakly H-bonded within the loop.

In contrast to T_7, the C_9 base moiety seems to be located in an isolated region outside of the loop. C_9 H6, H5, and H1′ signals exhibit NOEs only to other signals of the same nucleotide, with one exception (C_9 H6 → A_8 H4′). The pH dependence behavior of the C_9 H6 signal for Pt(en){d(ATGGGTACCCAT)} (Fig. 5) was different from that of the other C H6 signals, i.e. it shifted downfield from pH 7 to 4. This result demonstrates that C N3 is more easily protonated and is more accessible to solvent. The C_9 H6 signal was broadened at a lower Cu^{2+} concentration than the other C H6 signals [15]. This result demonstrates that N3 of C_9 is more accessible to Cu^{2+} than N3 of the base-paired C_{10} and C_{11} and is consistent with the isolated position of C_9.

^{31}P NMR results suggest a fairly strong distortion in the phosphate group 5′ to C_9. The far downfield shift of the ^{31}P signal of this phosphate group indicates a significant opening of the O-P-O bond angle [34]. The chemical shift of the phosphate group 3′ of C_9 is normal. The $^3J_{H3'-P}$ value for the 5′ phosphorus (Table 1) is typical of single-stranded DNA [30]. The ^{31}P–H3′ coupling constant for the 3′ phosphorus is unusually large, consistent with an increase in the C4′-C3′-O3′-P torsional angle. A similar result was obtained for the distorted region of *cis*Pt(NH_3)$_2${d(TCTCGGTCTC)-N7(5),N7(6)}.

In initial studies leading to the proposal of Model

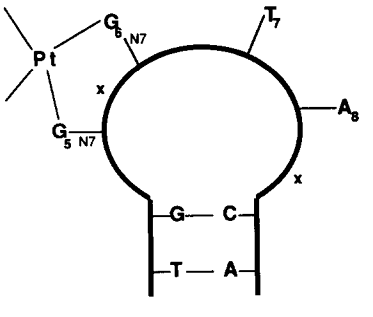

Model I

Fig. 7. Model I proposed for the structure of the TGGGTACCCA region of Pt(en){d(ATGGGTACCCAT)} and Pt(en){d(TATGGGTACCCATA)}. X indicates a phosphate group with an unusually shifted ^{31}P signal.

I [15, 17] (Fig. 7), it was assumed that Pt was bound to a GpG site, specifically G_5pG_6, due to the unusual position of that ^{31}P signal. Furthermore, the two downfield H8 signals are broad and exhibit a strong NOE to each other, two characteristics observed for H8 signals of Pt crosslinked guanine bases. However, 2D NMR results suggest that the more upfield of the two downfield signals is A_8. The furthest downfield H8 signal would then be G_5 or G_6. It must be emphasized that assignment of base proton signals depends on NOE crosspeaks. If some very unusual structure put the G_5 or G_6 H8 near the A_8 sugar, then A_8 H8 is the missing signal. However, this would require a second very unusual situation that the G_5 or G_6 H8 would not have any NOE crosspeaks to its own sugar. Therefore, the following discussion assumes the A_8 H8 assignment is correct.

Several possible modes of platination are being considered to evaluate the data we have collected on Pt(en){d(ATGGGTACCCAT)} and Pt(en){d(TATGGGTACCCATA)}. In our original Model I, described above, a normal G_5G_6 crosslink would explain the insensitivity of the G_5pG_6 ^{31}P signal to pH and temperature. The other unusual ^{31}P signals would be due to the unusual hairpin-like structure and thus would be sensitive to temperature and pH. The missing signal could be a consequence of broadening of an H8 due to a conformational process. Another explanation for the missing signal would be depurination caused by the platination reaction. However, digest analysis of the 14-mer after it had been platinated and then stripped of Pt by KCN revealed a ratio of 4A:4T:3G:3C, thereby eliminating the possibility of depurination. Furthermore, one consequence of depurination is to produce a mixture of α and β anomers of 2′-deoxyribose, which exist in a tautomeric equilibrium with the ring-opened aldehyde [35]. All H1′ signals are normal, also ruling out depurination.

However, Model I does not explain the strong NOE crosspeak between the two broad downfield H8 signals, $G_{(5 \text{ or } 6)}$ and A_8. Strong NOEs are usually observed between H8 signals of platinated purine bases [1, 13, 16]. Also, the A_8 H8 signal has characteristics typical of a platinated purine [8, 10, 12, 13, 16]. There are no reasons for believing that A H8 would be shifted downfield if it were not coordinated to Pt. Cu^{2+} binding studies provide supportive evidence that this signal is an A H8 [15]. Addition of Cu^{2+} to a solution of Pt(en){d(TATGGGTACCCATA)} resulted in broadening of this signal but not of the G_5 H8 signal. A possible reason for this result is Cu^{2+} binding at N1 of A and a contact (scalar) broadening effect on the H8 signal. N1 of G is not available for binding at pH 7. Therefore, Model I was abandoned.

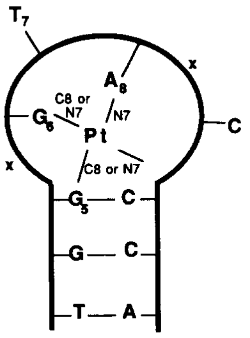

Model II

Fig. 8. Model II proposed for the structure of the TGGGTACCCA region of Pt(en){d(ATGGGTACCCAT)} and Pt(en){d(TATGGGTACCCATA)}. X indicates a phosphate group with an unusually shifted ^{31}P signal.

In a second type of model, Model II (Fig. 8), Pt is bound to three bases, G_5, G_6, and A_8. This would require displacement of one binding site of the en group or the formation of a five-coordinate complex. The pH and temperature insensitivity of the ^{31}P NMR signal of the G_5pG_6 are still explained by a direct effect of Pt crosslinking G_5 and G_6. The signal of the A_8pC_9 group, which is outside the Pt binding site, would be sensitive to disruption of secondary structure. The A_8 and one of the platinated G H8s would be brought close enough to account for the NOE between the two downfield signals. The other platinated G H8 signals could be missing for two possible reasons. First, the H8 is broadened by Pt binding at N7. Second, the free displaced end of the en group is situated near the H8 proton and catalyzes its exchange with H_2O.

In a variation of Model II, one of the G bases actually forms at Pt–C8 bond. This model, Model IIC (for carbon), could explain some of our data. It would explain the absence of one G H8 signal, whereas we find the H3′, H1′ and ^{31}P signals for all nucleotides. The problem with this model is that the en would have to dissociate at one end—a problem with Model II. The Pt—C bond would have to be labile to CN^- cleavage.

Two sets of results provide evidence against Model II. First, the ^{195}Pt NMR spectra of the 12-mer and the 14-mer have signals at −2645 and −2640 ppm respectively. These chemical shifts are similar to the reported shift for $[Pt(en)\{(Guo)_2\text{-}N7,N7\}]^{2+}$

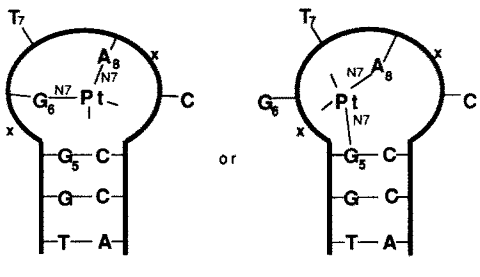

Model III

Fig. 9. Model III proposed for the structure of Pt(en){d(ATGGGTACCCAT)} and Pt(en){d(TATGGGTACCCATA)}. X indicates a phosphate group with an unusually shifted ^{31}P signal.

(−2662 ppm) [28]. This similarity strongly suggests that Pt is bound to two purine bases via N7. Binding to a C (such as C8 in Model IIC) would shift the ^{195}Pt NMR signal *ca.* 300 ppm upfield [36]. Second, upon addition of KCN and the resulting removal of Pt from Pt(en){d(ATGGGTACCCAT)}, the spectrum of the unreacted duplex was regenerated (Fig. 6). All 15 signals were present, indicating that the proton of the missing signal in Pt(en){d(ATGGGTACCCAT)}, or any moiety containing that proton, had not been physically removed from the oligonucleotide by platination. The presence of all signals in the D_2O solution (Fig. 6) also indicates that Pt does not bind at any C8 position.

We propose an alternative two-site binding model with A_8 and G_5 or G_6 bound to Pt, Model III (Fig. 9). Either possibility explains the downfield G_5pG_6 signal. If G_s is G_6, a downfield ^{31}P signal is expected since, in Z-DNA, the G residues exist in a *syn* conformation and the ^{31}P signals of the phosphate groups immediately 5′ to these residues are shifted downfield [34]. If G_s is G_5, the unusual position of the G_5pG_6 ^{31}P signal would be explained as a direct effect of Pt binding due to its location within the region bound by Pt.

G_5 binding is indicated by the lack of an upfield shift for T_7 H6 of the 12-mer between pH 8 and 10 (Fig. 5). Other results also suggest binding at G_5. First, the pH dependence study revealed an upfield shift for C_{10} H6 from pH 7.9 and 10.2. Assuming that G_s is G_5, this result could be explained by deprotonation of N1 H of G_5 (downfield shift of G_s H8 at *ca.* pH 8) and disruption of the G_5C_{10} base pair. Second, since G_s is bound to Pt, we expect a decreased pK_a to ~8. A pK_a of ~9.5 was actually observed. However, if the G is hydrogen-bonded to C_{10}, as G_5 is, the pK_a will be higher.

A possible explanation for the missing H8 signal is that the Pt moiety is close to the H8 proton, resulting in a large change in chemical shift for that proton signal. Librational effects would result in severe broadening of this ^{1}H signal so that it is not observable. In particular, NOEs were observed between the imino signal of G_4C_{11} (within the base stem) and signals of C_9 H6, G_s H8, and G_m H1′ in 1D NOE studies. NOEs were also observed between A_8 H8 and G_5C_{10} and between C_{11} NH_a and A_8 H2.

In summary, we have presented three possible models to explain the results we have obtained on this system. We feel, however, that Model III in which Pt is bound to G_5 and A_8 is the most reasonable. The regions T_1 through G_5 and C_{10} through A_{14} base pair with each other to form the stem region. The T_7 base moiety is located within the loop region and is in close proximity to both G_5 and G_6 nucleotides. The C_9 base moiety is forced out of the loop. G_5 exists in a *syn* conformation. The loop region may bend over, bringing some protons in this region into close proximity to some stem region protons.

Acknowledgements—This work was supported by NIH Grant GM29222 to L.G.M. The 500-MHz NMR instrument was funded in part by grants from the National Institutes of Health and the National Science Foundation.

REFERENCES

1. Reedijk J, Fichtinger-Schepman AMJ, van Oosteroom AT and van de Putte P, Platinum amine coordination compounds as anti-tumor drugs. Molecular aspects of the mechanism of action. *Structure Bonding* **67**: 53–89, 1987.
2. Marzilli LG, Kline TP, Live D and Zon G, ^{13}P NMR spectroscopic investigations of Pt-anticancer drug binding to oligonucleotide models of DNA, the probable molecular target. In: *Metal–DNA Chemistry* (Ed. Tullius T), pp. 119–145. American Chemical Society, Washington, DC, 1989.
3. Kline TP, Marzilli LG, Live D and Zon G, Investigations of Pt amine induced distortions in single- and double-stranded oligodeoxyribonucleotides. *J Am Chem Soc* **111**: 7057–7068, 1989.
4. Byrd RA, Summers MF, Zon G, Fouts CS and Marzilli LG, A new approach for assigning ^{31}P NMR signals and correlating adjacent nucleotide deoxyribose moieties via ^{1}H-detected multiple-quantum NMR. Application to the adduct of d(TGGT) with the anticancer agent, (ethylenediamine)dichloroplatinum. *J Am Chem Soc* **108**: 504–505, 1986.
5. Wilson WD, Heyl BL, Reddy R and Marzilli LG, Diagmagnetic metal species that induce pronounced changes in the ^{31}P NMR spectrum of DNA. *Inorg Chem* **21**: 2527–2528, 1982.
6. Marzilli LG, Reily MD, Heyl BL, McMurray CT and Wilson WD, Evidence for similar structural changes on binding of platinum anti-tumor agents to DNA and nucleosomes. *FEBS Lett* **176**: 389–392, 1984.
7. den Hartog JHJ, Altona C, van Boom JH and Reedijk J, A phosphorus NMR study of the reaction products of *cis*-diamminedichloroplatinum(II) with a double-helical oligonucleotide and with DNA. *FEBS Lett* **176**: 393–397, 1984.
8. Reily MD and Marzilli LG, ^{31}P and ^{1}H NMR spectroscopic studies of platinum adducts of poly(I)·poly(C). The antitumor agent *cis*-$Pt(NH_3)_2Cl_2$ forms an N7,N7 bis-adduct. *J Am Chem Soc* **107**: 4916–4924, 1985.
9. Fouts CS, Reily MD, Marzilli LG and Zon G, ^{31}P NMR investigation of fourteen self-complementary oligodeoxyribonucleotides (8-mer to 14-mer) treated with platinum complexes: The downfield ^{31}P NMR signal characteristic of anti-cancer drugs is observed only for molecules with adjacent G residues. *Inorg Chim Acta* **137**: 1–13, 1987.
10. den Hartog JHJ, Altona C, van der Marel GA and

Reedijk J, A ^{1}H and ^{31}P NMR study of *cis*-Pt(NH$_3$)$_2$[d(CpGpG)-N7(2),N7(3)]. The influence of a 5′-terminal cytosine on the structure of the *cis*-Pt(NH$_3$)$_2$[d(GpG)-N7,N7] intrastrand crosslink. *Eur J Biochem* **147**: 371–379, 1985.

11. den Hartog JHJ, Altona C, Chottard J-C, Girault J-P, Lallemand J-Y, de Leeuw FAAM, Marcelis ATM and Reedijk J, Conformational anslysis of the adducts *cis*-{Pt(NH$_3$)$_2${d(GpG)}}$^+$ in aqueous solution. A high field (500–300 MHz) nuclear magnetic resonance investigation. *Nucleic Acids Res* **10**: 4715–4730, 1982.
12. van der Veer JL, van der Marel GA, van den Elst H and Reedijk J, The antitumor drug *cis*-diamminedichloroplatinum(II) preferentially chelating neighboring guanines in the trinucleotide d(pGpGpG). *Inorg Chem* **26**: 2272–2275, 1987.
13. Fouts CS, Marzilli LG, Byrd RA, Summers MF, Zon G and Shinozuka K, HMQC and ^{1}H and ^{31}P NMR studies of platnium amine adducts of tetradeoxyribonucleotides. Relationship between ^{31}P shift and potential hydrogen-bonding interactions in pGpG moieties cross-linked by platinum. *Inorg Chem* **27**: 366–376, 1988.
14. Caradonna JP and Lippard SJ, Synthesis and characterization of [d(ApGpGpCpCpT)]$_2$ and its adduct with the anticancer drug *cis*-diamminedichloroplatinum(II). *Inorg Chem* **27**: 1454–1466, 1988.
15. Fouts CS, *anti-cancer drug interactions with oligodeoxyribonucleotides*. Ph.D. Thesis, Emory University, 1987.
16. den Hartog JHJ, Altona C, van Boom JH, van der Marel G, Haasnoot CAG and Reedijk J, *cis*-Diamminedichloroplatinum(II) induced distortion of a single and double stranded deoxydecanucleosidenonaphosphate studied by nuclear magnetic resonance. *J Biomol Struct Dyn* **2**: 1137–1155, 1985.
17. Marzilli LG, Fouts CS, Kline TP and Zon G, Unusual hairpinlike conformations of oligonucleotides induced by platinum anti-cancer drugs. In: *Platinum and Other Metal Coordination Compounds in Cancer Chemotherapy* (Ed. Nicolini M), pp. 67–73. Martinus Nijhoff, Boston, 1987.
18. Eadie JS, McBridge LJ, Efcavitch JW, Hoff LB and Cathcart R, High-performance liquid chromatographic analysis of oligodeoxyribonucleotide base composition. *Anal Biochem* **165**: 442–447, 1987.
19. Bax A, Griffey RH and Hawkins BL, Correlation of proton and nitrogen-15 chemical shifts by multiple quantum NMR. *J Magn Reson* **55**: 301–315, 1983.
20. Sklenar V and Bax A, Measurement of ^{1}H-^{31}P NMR coupling constants in double-stranded DNA fragments. *J Am Chem Soc* **109**: 7525–7526, 1987.
21. Sklenar V, Miyashiro H, Zon G, Miles HT and Bax A, Assignment of the phosphorus-31 and proton resonances in oligonucleotides by two-dimensional NMR. *FEBS Lett* **208**: 94–98, 1984.
22. Jeener J, Meier BH, Bachmann P and Ernst RR, Investigation of exchange processes by two-dimensional NMR spectroscopy. *J Chem Phys* **71**: 4546–4553, 1979.
23. Wüthrich K, *NMR of Proteins and Nucleic Acids*. John Wiley, New York, 1986; and references contained therein.
24. Early TA, Kearns DR, Hillen W and Wells RD, A 300-MHz proton nuclear magnetic resonance investigation of deoxyribonucleic acid restriction fragments. Dynamic properties. *Biochemistry* **20**: 3764–3769, 1981.
25. Patel DJ, Proton and phosphorus NMR studies of d-CpG(pCpG)$_n$ duplexes in solution. Helix-coil transition and complex formation with actinomycin-D. *Biopolymers* **15**: 533–558, 1976.
26. Patel DJ, Shapiro L and Hare D, DNA and RNA: NMR studies of conformations and dynamics in solution. *Q Rev Biophys* **20**: 35–112, 1987.
27. Lankhorst PP, Haasnoot CAG, Erkeleus C and Altona C, Carbon-13 NMR in conformational analysis of nucleic acid fragments. 2. A reparametrization of the Karplus equation for vicinal NMR coupling constants in CCOP and HCOP fragments. *J Biomol Struct Dyn* **1**: 1387–1405, 1984.
28. Miller SK and Marzilli LG, Interaction of platinum antitumor agents with guanine nucleosides and nucleotides. ^{195}Pt and ^{1}H NMR spectroscopic characterization of compound III. *Inorg Chem* **24**: 2421–2425, 1985.
29. Marzilli LG, Hayden Y and Reily MD, First definitive demonstration of ortho shielding effects on ^{195}Pt NMR signals. Dependence of shift on heterocyclic ligand basicity and ortho substituents in four series of complexes with chloro, dimethyl sulfoxide, and pyridine ligands. *Inorg Chem* **25**: 974–978, 1986.
30. Altona C, Conformational analysis of nucleic acids. Determination of backbone geometry of single-helical RNA and DNA in aqueous solution. *Recl: J.R. Neth Chem Soc Rev* **101**: 413–433, 1982.
31. Gorenstein DG, Schroeder SA, Fu JM, Metz JT, Roongta V and Jones CR, Assignments of ^{31}P NMR resonances in oligodeoxyribonucleotides. Origin of sequence-specific variations in the deoxyribose phosphate backbone conformation and the ^{31}P chemical shifts of double-helical nucleic acids. *Biochemistry* **27**: 7223–7237, 1988.
32. Altona C, Versatile oligonucleotides: B DNA, Z DNA, and DNA hairpins as seen in aqueous solution by two-dimensional NMR. *Nucleosides Nucleotides* **6**: 157–172, 1987.
33. Hare DR and Reid BR, Three-dimensional structure of DNA hairpin in solution: Two-dimensional NMR studies and distance geometry calculations on (dCGCGTTTTCGCG) *Biochemistry* **25**: 5341–5350, 1986.
34. Gorenstein DG (Ed), *Phosphorus-31 NMR*. Academic Press, New York, 1984; and references contained therein.
35. Basu AK and Essigman JM, Site-specifically modified oligodeoxynucleotides as probes for the structural and biological effects of DNA-damaging agents. *Chem Res Toxicol* **1**: 1–18, 1988.
36. Hollis LS, Stern EW, Amundsen AR, Miller AV and Doran SL, Platinum complexes of vitamin C. NMR studies on the solution chemistry of *cis*-Pt(diamine)(ascorbate) complexes. *J Am Chem Soc* **109**: 3596–3602, 1987.